Submarine landform assemblages and sedimentary processes in front of Spitsbergen tidewater glaciers

Katharina Streuff[a,*], Colm Ó Cofaigh[a], Riko Noormets[b], Jeremy Lloyd[a]

[a] *Durham University, Department of Geography, South Road, Durham DH1 3LE, United Kingdom*
[b] *The University Centre in Svalbard (UNIS), P.O. Box 156, N-9171 Longyearbyen, Norway*

Abstract

New swath-bathymetric data from the inner parts of the three Svalbard fjords Ymerbukta, Trygghamna, and Magdalenefjorden reveal the landform assemblages deposited in front of tidewater glaciers in west and northwest Spitsbergen. Overridden moraines in Ymerbukta, a tributary of Isfjorden in central west Spitsbergen, record several re-advances of the Esmarkbreen glacier at the head of the fjord after deglaciation, and glacial lineations formed in seafloor sediments are indicative of fast ice advance during one of these events. A terminal moraine and associated debris lobe mark the maximum ice extent during the Holocene, which, implied by the presence of crevasse-squeeze ridges, is likely related to a surge of Esmarkbreen. Several De Geer moraines provide evidence for subsequent slow and step-wise retreat. In the adjacent Trygghamna and in Magdalenefjorden in northwest Spitsbergen the landforms are similar but the absence of overridden moraines and glacial lineations shows that the glaciers probably only re-advanced once during the Holocene and that ice flow was relatively slow. Terminal moraines and associated debris lobes mark the maximum extent of these advances and formed during the Little Ice Age (LIA). In Mag-

*Corresponding author

Email addresses: katharina.streuff@durham.ac.uk (Katharina Streuff), colm.ocofaigh@durham.ac.uk (Colm Ó Cofaigh), riko.noormets@unis.no (Riko Noormets), j.m.lloyd@durham.ac.uk (Jeremy Lloyd)

dalenefjorden the relatively small size of the debris lobe suggests that the ice margin was at its maximum position for only a short period of time, or that sediment availability was restricted during the LIA advance. Similar to Esmarkbreen the retreat phase of the glaciers in Trygghamna and Magdalenefjorden was also characterised by periods of still-stand or small re-advances, although the comparatively small number of De Geer moraines in all three fjords shows that these landforms probably formed much less frequently than previously thought. Sub-bottom profiler data, four sediment cores and six radiocarbon dates from Magdalenefjorden further provide information about the Holocene sedimentary environments in a northwest Spitsbergen fjord. The main source of sediment is glacial meltwater entering the fjord from the surrounding coastline, which has led to the accumulation of thick sequences of fine-grained mud. Stratified and laminated muds record glacier-proximal conditions, probably related to a LIA re-advance of Waggonwaybreen around 300 cal a BP, where the interplay of a range of glacimarine processes led to the formation of partially rhythmic couplets of one coarser and one finer layer, accumulated at a rate of around 3 cm a^{-1}. Multiple sandy layers intercalated with the glacimarine mud provide evidence for the occurrence of gravitational mass-flow events like turbidity currents. In ice-distal settings, massive to weakly stratified, occasionally bioturbated mud accumulated at a lower rate of 0.04–0.49 cm a^{-1}. Occasional clasts and diamictic layers show that the depositional environment in Magdalenefjorden is also influenced by sedimentation from icebergs and sea ice, but the ubiquitous glacimarine mud underscores the predominance of meltwater-related sedimentation in the fjord.

Keywords: Fjords, glacial sediments, submarine landforms, west Spitsbergen, Holocene, ice retreat

1. Introduction

High-Arctic glaciers have received increasing attention in the scientific literature as their behaviour is often closely linked to climate change (e.g. Lovell, 2000; Holland et al., 2008; Błaszczyk et al., 2009). In this context, Svalbard has been of particular interest, as around 60% of the archipelago is still covered by glaciers, many of which reach tidewater (e.g. Hagen, 1993; Hagen et al., 2003; Kohler et al., 2007; Mangerud & Landvik, 2007). The ongoing thinning and retreat of these glaciers has resulted in the exposure of well-preserved glacial landform-sediment assemblages in many fjords (e.g. Plassen et al., 2004; Ottesen et al., 2008; Fransner et al., 2017; Streuff et al., 2017), which generally include glacial lineations, terminal moraines marking the maximum extent of ice advance, debris lobes on the distal flanks of the terminal moraines, and recessional moraines or annual push moraines (e.g. Boulton et al., 1996; Plassen et al., 2004; Forwick & Vorren, 2011; Flink et al., 2015; Streuff et al., 2015). Eskers, bedrock highs, crevasse-squeeze ridges, iceberg ploughmarks and pockmarks have further been documented from individual fjords (e.g. Ottesen & Dowdeswell, 2006; Ottesen et al., 2008; Forwick et al., 2009; Dowdeswell & Ottesen, 2016; Flink et al., 2017; Streuff et al., 2017).

The landforms and sediments deposited in front of Svalbard tidewater glaciers serve as an important indicator of past ice dynamics and have led to a better understanding not only of the response of the Svalbard-Barents Sea Ice Sheet (SBIS) to climate change since the Last Glacial Maximum (LGM), but also of individual glacier dynamics throughout the Holocene. The latter are of particular importance for future predictions of the cryosphere as tidewater glaciers can exhibit a wide range of hydrological, thermal, and dynamic regimes (e.g. Blatter & Hutter, 1991; Dowdeswell et al., 1998; Pettersson, 2004). The present study aims to elucidate the individual tidewater glacier dynamics in three Spitsbergen fjords, two in central west Spitsbergen, and one in northwest Spitsbergen, by using new swath-bathymetric data from the inner fjord basins; it thereby further contributes to the knowledge we have of the glaciation history of the SBIS. Based on the swath-bathymetric data, we identify the landform assemblages in these fjords and thus complement the work of Forwick et al. (2009), Ottesen & Dowdeswell (2009), and Forwick & Vorren (2012), who documented the landforms in the outer fjord basins. We further use sub-bottom profiler and lithological data, including radiocarbon dates, from Magdalenefjorden to correlate landforms with the sedimentary facies and to reconstruct glacimarine sedimentary processes and associated accumulation rates. Combined, our data enable us to reconstruct the Holocene depositional processes and products in front of selected Spitsbergen tidewater glaciers, to compare and contrast them with those from other glacimarine environments on Svalbard, and thus to evaluate the importance of regional versus local controls on individual glacier dynamics.

2. Study Areas

2.1. Physiographic Setting

Three fjords were investigated: Ymerbukta, Trygghamna, and Magdalenefjorden (Figs. 1, 2). They are located on Spitsbergen, the largest island of the Svalbard archipelago. Their physiographic details are summarised in Table 1. Ymerbukta and Trygghamna in central west Spitsbergen are northern tributaries of Isfjorden, which, together with its many tributaries, forms Svalbard's largest fjord system (Fig. 1b). Ymerbukta and Trygghamna extend approximately north to south, with the former fjord located east and the latter west of the mountain range Värmlandryggen (Fig. 2a). Both fjords are separated

Table 1: Physiographic details of the fjords from the study area. Local glaciers are listed in the last column with (m) = marine-terminating/tidewater and (t) = terrestrial glaciers. For more details see also Figure 2.

Fjord	**Latitude**	**Longitude**	**Width [m]**	**Length [km]**	**Depth [m]**	**Glaciers**
Ymerbukta (inner basin)	78°16'30"N–78°18'00"N	13°52'E–14°05'E	500–1600	3.5	10–85	Esmarkbreen (m)
Ymerbukta (outer basin)	78°12'00"N–78°16'30"N	13°52'E–14°05'E	1300–2800	6.5	20–160	
Trygghamna (inner basin)	78°14'30"N–78°16'30"N	13°38'E–13°52'E	800–1800	2.4	2–35	Kjerulfbreen (m) Harrietbreen (m)
Trygghamna (outer basin)	78°12'00"N–78°15'30"N	13°38'E–13°52'E	1500–2400	5.5	30–180	Protektorbreen (t) Alkhornbreen (t)
Magdalenefjorden (inner basin)	79°32'30"N–79°33'30"N	11°08'E–11°18'E	700	2.5	40–110	Waggonwaybreen (m) Miethebreen (t)
Magdalenefjorden (central basin)	79°33'00"N–79°34'30"N	10°55'E–11°05'E	800–1400	4.5	50–140	Brokebreen (t) Buchanbreen (t)
Magdalenefjorden (outer basin)	79°33'00"N–79°36'00"N	10°45'E–10°55'E	900–4500	7.3	25–95	Adambreen (t) Skarpeggbreen (t)

into an inner, ice-proximal and an outer, ice-distal basin by a prominent ridge (Table 1, Fig. 2a).

Magdalenefjorden is located in northwest Spitsbergen (Table 1, Fig. 2b). It is orientated southeast to northwest and can be subdivided into an innermost ice-proximal basin, a deep central basin and an outer, ice-distal basin (Table 1, Fig. 2b). Along its southern coast Magdalenefjorden is joined by a small tributary fjord, Gullybukta, which hosts the glacier Gullybreen at its head (Fig. 2b).

2.2. Previous Work

2.2.1. Glacial Background

During the LGM Svalbard was covered by a large and dynamic ice sheet, which reached the continental shelf edge and was divided into two components: (1) fast-flowing ice streams draining the ice sheet through the major fjord systems, and (2) "inter-ice-stream" areas of slower-moving ice (Elverhøi et al., 1995; Landvik et al., 1998; Ottesen et al., 2007; Ingólfsson & Landvik, 2013). Isfjorden and its tributaries likely served as a major pathway for one of these large ice streams, with ice reaching its maximum extent at the continental shelf edge between 24 and 20 ka BP (e.g. Mangerud et al., 1992; Svendsen et al., 1992; Landvik et al., 1998, 2005; Ottesen et al., 2005; Jessen et al., 2010). Ice retreated rapidly from ∼14.8 ka BP until ∼12.3 ka BP, by which time Isfjorden's coastal areas were ice-free (Mangerud et al., 1992; Elverhøi et al., 1995; Svendsen et al., 1996; Landvik et al., 1998). A re-advance occurred around 12.4 ka BP, after which ice retreated to the heads of the tributary fjords until ∼10 ka BP (e.g. Landvik et al., 1995; Ottesen et al., 2007; Forwick & Vorren, 2009). Geomorphological evidence from Ymerbukta and Trygghamna, as well as lithological evidence from elsewhere in the Isfjorden fjord system, suggest that the glaciers underwent a significant re-advance during the Younger Dryas (Mangerud et al., 1992; Svendsen et al., 1996; Forwick & Vorren, 2009, 2011), which is in contrast to other areas in Spitsbergen where glaciers were smaller during the Younger Dryas than during the LIA (Mangerud & Landvik, 2007). In the Isfjorden system, the glaciers experienced asynchronous regrowth after c. 9 ka BP (e.g. Forwick & Vorren, 2007, 2009; Baeten et al., 2010; Forwick et al., 2010), and their maximum Holocene extents occurred in response to the LIA cooling or due to climatically independent surges (e.g. Plassen et al., 2004; Ottesen & Dowdeswell, 2006; Mangerud & Landvik, 2007; Forwick & Vorren, 2011).

In contrast to Isfjorden, Magdalenefjorden was located in an inter-ice-stream area during the LGM, with ice streams located south and east of the fjord, in Kongsfjorden and Woodfjorden (Fig. 1b; e.g. Landvik et al., 2005; Ottesen & Dowdeswell, 2009). Ice flow in Magdalenefjorden was inferred to be relatively slow due to a more alpine topography in the coastal areas, a thinner ice cover and generally reduced ice flux (e.g. Landvik et al., 1998; Forman, 1990; Landvik et al., 2003, 2005; Ottesen & Dowdeswell, 2009). A grounding zone wedge close to the continental shelf edge provides evidence that, similar to west Spitsbergen, ice in the northwest reached the shelf edge during the LGM (Ottesen & Dowdeswell, 2009). The timing of ice retreat from the shelf edge is still very poorly understood. The only constraints on deglaciation are ^{10}Be exposure dates from the lowlands of the two islands Amsterdamøya and Danskøya (Fig. 1), which suggest that these areas were ice-free between 18 and 15 ka BP (Landvik et al., 2005). This may indicate that the mouth of Magdalenefjorden deglaciated around the same time, suggesting that it was probably ice-free much earlier than Isfjorden. Indeed, early deglaciation of northwest Svalbard was also suggested by Forman (1990) and is further supported by Koç et al. (2002) who placed the disintegration of the northern margin of the Svalbard-Barents Sea Ice Sheet in northeast Spitsbergen between 13.9 and 13.7 ka BP. From the geomorphological evidence ice retreat was inferred to be continuous and relatively rapid across the outer shelf, and slower but quasi-continuous across the inner shelf (Ottesen et al., 2007; Ottesen & Dowdeswell, 2009). It is unclear when Magdalenefjorden was deglaciated and the local tidewater glaciers reached the head of the fjord, but a minimum deglaciation age of 8.9–8.5 ka BP from the mouth of the adjacent Smeerenburgfjorden may serve as a rough estimate (Velle, 2012).

2.2.2. Geomorphology

Previous work has been carried out on the landforms in the outer parts of all three fjords. In outer Ymerbukta Forwick et al. (2009) documented the abundance of single and composite pockmarks, which were described as up to 250 m wide and 7 m deep. The pockmarks were inferred to have formed from the upward seepage of thermogenic gas, probably predominantly along tectonic faults occurring in the Isfjorden-Ymerbukta Fault Zone (Dallmann et al., 2002; Forwick et al., 2009). Indeed, systematic analysis of seafloor seepage features in the entire Isfjorden fjord system linked the occurrence of pockmarks to the presence of deep bedrock faults and igneous intrusions (Senger et al., 2013; Roy et al., 2015). Further work by Forwick & Vorren (2012) has shown the presence of several sediment lobes, as well as blocks and flow structures in both Ymerbukta and Trygghamna. The majority of the sediment lobes occur in Ymerbukta, are orientated perpendicular to the main fjord axis, and were described as up to 5-m thick and up to 500-m long and wide deposits. In Trygghamna, where the presence of sediment lobes is less common, two areas with slide blocks were identified, where individual blocks are up to 150 m wide, up to 100 m long, and up to 8 m high (Forwick & Vorren, 2012). The sediment lobes and slide blocks were inferred to represent debris-flow deposits or slump/slide deposits, formed from slope failure during the late Holocene with earthquakes and high sediment accumulation rates as the most likely triggers (Forwick & Vorren, 2012). The presence of terminal moraines, marking the Holocene maximum extent of the local glaciers in Ymerbukta and Trygghamna, was also indicated by Forwick & Vorren (2012). Large sediment lobes on their distal flanks were interpreted as glacigenic debris flows formed from high sediment supply to the glacier margin, causing repeated slope failure during a period of still-stand.

Ottesen & Dowdeswell (2009) described the seafloor of Magdalenefjorden as generally smooth, and related this to sediment infill and draping by silt and clay settling from suspension in glacial meltwater plumes, with the occurrence of occasionally protruding bedrock in the form of ridges and knobs. On the steep side walls of the central fjord basin the same authors described the occurrence of scars and possibly gullies. In the outer fjord, arcuate sedimentary ridges have a SW-NE orientation and were identified as moraines formed at the retreating ice margin during periods of still-stand (Ottesen & Dowdeswell, 2009). A 40 m high ridge across the central fjord was interpreted as the terminal moraine marking the maximum extent of Waggonwaybreen during the LIA, which occurs in conjunction with several up to 5 m high transverse ridges, interpreted as push moraines. The latter are thought to form regularly, possibly annually, during small re-advances of the glacier front during overall ice retreat (Ottesen & Dowdeswell, 2009). The same processes were inferred for a number of similar ridges in front of Gullybreen along the southern shore of the fjord (Ottesen & Dowdeswell, 2009).

2.2.3. Seismostratigraphy

While sub-bottom profiler data and sediment cores are available for Magdalenefjorden, and will be investigated here, the seismostratigraphy in Ymerbukta and Trygghamna is derived from seismic interpretations published by Forwick & Vorren (2011, 2012), which were based on a chirp profile through Ymerbukta (F04-017; Fig. 2a), and a boomer profile through Trygghamna (SB-04-023 in Fig. 2a; for details see Fig. 63.3 in Forwick & Vorren (2012) and Fig. 4b in Forwick & Vorren (2011)). In addition to the acoustic basement, interpreted as bedrock, four acoustic units were described from the two fjords: S2, S4a, S5 and S6 (Forwick & Vorren, 2011, 2012). In Isfjorden, at the mouth of the two fjords, two additional units, S1 and S3, occur.

Unit S1 was described as (semi-)transparent with few internal reflections and a smooth to hummocky upper boundary. It has a draping character, occurs as basin-fill and on bathymetric slopes, and is present on top of the bedrock in most of Isfjorden (Forwick & Vorren, 2011). The unit was inferred to represent sediment deposited subglacially as till or as cavity infill, with a hummocky appearance ascribed to the presence of glacial lineations (Forwick & Vorren, 2011). The acoustically massive (semi-)transparent unit S2 was determined to represent push or thrust moraines accumulating at the glacier front during recession or minor re-advances during deglaciation, which were inferred to be indicative of episodic retreat (Forwick & Vorren, 2011). Unit S3 appears as mostly wedge-shaped deposits of a stratified to chaotic acoustic appearance (Forwick & Vorren, 2011). The wedges are usually orientated parallel to the direction of (paleo-) ice flow and were interpreted as products of (1) glacial outwash, (2) repeated slope failures caused by high sedimentation rates, isostatic uplift and seismic activity, or (3) the infill of subglacial cavities (Forwick & Vorren, 2011). The acoustically stratified deposits of unit S4a are characterised by a draping or onlapping geometry and (sub-)parallel internal reflections, and are up to 38 and 40 m thick in Ymerbukta and Trygghamna, respectively (Forwick & Vorren, 2011). S4a was found to correlate with stratified glacimarine mud with sandy beds and clasts, which were derived from suspension settling from meltwater, ice rafting, and mass-transport activity in a glacier-proximal environment. The unit probably dates back to the Younger Dryas and was deposited between 14.1 and 11.2 cal ka BP (Forwick & Vorren, 2009, 2011). Unit S5 represents glacimarine deposits from the Early Holocene, which are acoustically (semi-)transparent, conformably overlie S4a, and show occasional onlap geometry. The sediments were sourced from suspension settling and occasional iceberg rafting during the Holocene Thermal Optimum between 11.2 and 9 cal ka BP (Forwick & Vorren, 2009, 2011). Unit S6 is the stratigraphically youngest facies in Ymerbukta and Trygghamna. It is acoustically stratified and interpreted as Holocene glacimarine pebbly mud deposited after ~9 cal ka BP, when ice rafting increased due to colder climatic conditions (Forwick & Vorren, 2009, 2011).

3. Methods

For this study, swath-bathymetric data from Magdalenefjorden, Ymerbukta, and Trygghamna were supplemented with sub-bottom profiler data and four sediment cores from Magdalenefjorden. The data from Magdalenefjorden were gathered in October 2009 on the research vessel *R/V Jan Mayen* (now *Helmer*

Hanssen), using a Kongsberg Simrad multibeam EM300 echo sounder for the swath-bathymetric, and an EdgeTech 3300-HM sub-bottom profiler for the chirp data. Swath-bathymetric data from Ymerbukta and Trygghamna were gathered in July 2000 by the Norwegian Hydrographic Survey with a Kongsberg Simrad multibeam EM1002 installed on the research vessel *Sjømaleren* (now *IXPLORER*). Both multibeam echo sounders were calibrated using frequent conductivity-temperature-depth (CTD) measurements from the water column. Bathymetric data were gridded to a cell size of 5x5 m in DMagic, and visualised and interpreted in the Fledermaus v7 3D Software. The chirp sub-bottom profiler was operating at a pulse mode of 2–16 kHz and 3 ms during acquisition and the resulting data were processed using the EdgeTech Software and visualised and interpreted in the Kingdom Suite software. Generally assuming water-saturated sediments, an average p-wave velocity of 1500 m s^{-1} was used for the correlation between seismo- and lithostratigraphy, i.e. conversion from ms to m.

A total of four gravity cores, JM09H-GC01, GC03, GC06, and GC09, were taken from Magdalenefjorden, using a 1900 kg heavy gravity corer with a 6 m long steel barrel and an inner diameter of ∼110 mm. All cores were cut into sections up to 1.3 m in length, split into working and archive halves, and stored at +4°C. It is important to note that GC01 and GC03 were split in 2009, whereas GC06 and GC09 were split in 2016. Thus, certain parameters (e.g. water content) may not be directly comparable between the four cores, although variations within one core are informative. In order to identify the different lithofacies in the fjord, core logs were generated from the visual description of the sediment surface of the working halves, which were supplemented using the information on internal sedimentary structures provided by x-radiographs. The latter were acquired with a GEOTEK Thermo Kevex PSX10-65W-Varian2520DX, running with a voltage of ~95 kV and a current of around 150 nA. All cores were run through a GEOTEK multi-sensor core logger at Durham University to determine the wet-bulk density and magnetic susceptibility in 1 cm intervals, the latter of which was measured with a Bartington point-sensor mounted on the system. Magnetic susceptibility values were obtained in SI units (χ x 10^{-5}) but are displayed unitless throughout this article. Bivalve shells located from the x-rays of GC06 and benthic foraminifera from selected sediment depths in GC01 were sent to Beta Analytic for Accelerator Mass Spectrometry (AMS) dating. The obtained conventional ^{14}C ages were calibrated with the MARINE13 calibration (cf. Reimer et al., 2013), using a marine reservoir effect of 400 years and a local ΔR of 61 $\pm$ 70 years (Mangerud, 1972). For the water content 1 cm thick sediment slabs were taken at selected (usually lithofacies-dependent) core depths, weighed, dried at 60°C, and weighed again. The same samples were subsequently soaked overnight in a solution of distilled water and sodium-hexametaphosphate to encourage the disintegration of flocculated clay particles. The sediments were then sieved through mesh sizes of 500, 250, 125 and 63 μm (stacked on top of each other) to determine the grain size distribution within the cores.

4. Results

4.1. Geomorphology

Based on the swath-bathymetric data from the inner parts of Ymerbukta, Trygghamna, and Magdalenefjorden we identify a total of five different landform types. The distribution of all observed landforms is shown in Fig. 3, which incorporates those landforms previously described by Forwick et al. (2009), Ottesen & Dowdeswell (2009), and Forwick & Vorren (2012).

Groove-ridge features – glacial lineations

Elongate, (sub-)parallel ridges and grooves are present in inner Ymerbukta (Fig. 4a, b). These features are 25 m high, 150–800 m long, up to 20 m wide and spaced at irregular distances between 50 and several hundred meters (Fig. 4a, b). The crests are straight to slightly curved, and round and symmetrical in cross-section. These ridges are orientated parallel to the main fjord axis, i.e. in the direction of ice flow (Fig. 3b). The majority of these features are overprinted by transverse ridges (see section 4.1 below), indicating that the elongate ridges were deposited first. Similar, albeit larger ridges (up to 2 km long, ∼200 m wide) appear in Isfjorden, where their orientation is northeast-southwest, i.e. almost normal to the ridges in Ymerbukta (Fig. 3b).

Similar sets of ridges and grooves have previously been described from other Spitsbergen fjords, where they were interpreted as glacial lineations (e.g. Ottesen & Dowdeswell, 2006; Ottesen et al., 2008; Streuff et al., 2015). Indeed, Ottesen et al. (2007) documented the presence of (mega-scale) glacial lineations in Isfjorden. Glacial lineations are formed beneath a glacier or ice stream, where the soft subglacial sediments are deformed into ridges and grooves by processes of erosion and re-deposition (e.g. Tulaczyk et al., 2001; Ó Cofaigh et al., 2005). They are commonly associated with fast ice flow (King et al., 2009).

Transverse ridges – recessional moraines

Several large ridges in the innermost fjord basins are orientated transverse to the main fjord axis (Figs. 3, 4) and extend across the width of the fjords. The ridges are up to 20 m high, 800–2000 m long and 100–300 m wide. Their sometimes multiple crests are sinuous in planform, round, and mostly symmetrical in cross-section (Fig. 4d, f). In Ymerbukta some of these ridges are overprinted by the glacial lineations. The most distal ridges in Ymerbukta and Trygghamna are associated with large sediment lobes (see section 2.2.2), which extend down their distal flanks (Fig. 3b). In Isfjorden a large feature occurs, which is similar to the transverse ridges in the fjords, but is ∼85 m high, ∼4 km wide and more than 3.8 km long (Fig. 4h-j). It is characterised by an asymmetric cross-profile with a steeper distal and a flatter proximal side (Fig. 4). In plan-view, it appears more as a plateau with a sharp edge rather than a ridge with a crest (Figs. 3a, b, 4).

The large transverse ridges are interpreted to be recessional moraines deposited during overall glacier retreat. This is in accordance with e.g. Ottesen & Dowdeswell (2006), Baeten et al. (2010) and Streuff et al. (2015), who described similar ridges from other Spitsbergen fjords. In Ymerbukta, where these ridges are partially streamlined or overprinted by glacial lineations, they probably represent recessional moraines from an earlier advance of Esmarkbreen, that were overprinted by a later re-advance. The transverse ridges at the outermost edge of the inner basins in Ymerbukta, Trygghamna, and Magdalenefjorden have previously been interpreted as terminal moraines, deposited when the glaciers reached their maximum Holocene extents, either in response to the LIA cooling (Ottesen & Dowdeswell, 2009) or as a result of a surge (Forwick & Vorren, 2012).

We suggest that the ridge-like feature in Isfjorden formed as a sedimentary wedge at or close to the grounding line of an ice stream during a period of still-stand during overall ice retreat. Although formation as a grounding-zone wedge could be feasible in this context, a seismic profile across the feature (SS97-163; Fig. 4j) does not show the characteristic reflection pattern (cf. Forwick & Vorren, 2011; Batchelor & Dowdeswell, 2015). We thus support the interpretation of Forwick & Vorren (2011), who, from the seismic profile, inferred the formation of wedge-shaped ice-marginal deposits either from repeated slope failure, as glacial outwash or as sedimentary infill of subglacial cavities.

Small transverse ridges – De Geer moraines

Abundant small transverse ridges occur in the inner fjord basins, which extend across the fjords and are between 100 and 2000 m long, around 20 m wide, and ~3 m high. These ridges overprint the glacial lineations in Ymerbukta, indicating that they are the youngest features. The majority have sharply defined, continuous crests, are largely symmetrical in cross-section, and are spaced at intervals between 10 and 50 m (Fig. 4a, c). In places these ridges exhibit branching and may cross-cut each other (Fig. 3).

The small ridges are similar to annual push moraines described from other Svalbard fjords (e.g. Ottesen et al., 2008; Flink et al., 2015), which are formed each year during winter, when the presence of shore-fast sea ice causes the generally retreating glaciers to stagnate or even re-advance (Boulton, 1986; Ottesen & Dowdeswell, 2006). The overall regular spacing supports this interpretation. The fact that these ridges exhibit branching and cross-cut each other in places could be indicative of other processes involved, e.g. the squeezing of soft subglacial sediments into basal glacier crevasses (see Evans & Orton, 2014; Streuff et al., 2015). This is supported by the presence of terrestrial crevasse-squeeze ridges in the forefield of Esmarkbreen (Farnsworth et al., 2016). Given the likely mixed origin of the small ridges both as end moraines and as crevasse-squeeze ridges, we interpret these landforms as De Geer moraines (cf. Lundqvist, 1981; Streuff et al., 2015).

4.2. Seismostratigraphy

Description

The chirp data available from Magdalenfjorden reveal a total of five acoustic facies, AF1–AF5 (Fig. 5). Their characteristics are summarised in Table 2.

AF1 is the stratigraphically lowermost facies in Magdalenefjorden and is defined by very weak and chaotic internal reflections that disappear with depth and a discontinuous, often hummocky upper boundary (Table 2, Fig. 5). AF2 directly overlies AF1 in most of the fjord and has a similar acoustic signature to AF1 (Table 2, Fig. 5c). The top boundary of AF2 is usually strong and opaque and is sometimes accompanied by strong diffraction hyperbolae (Fig. 5c). AF3 conformably overlies AF2, or AF1, where AF2 is absent. Its acoustic

Table 2: Acoustic facies in Magdalenefjorden. An average p-wave velocity of 1500 m s^{-1} was used to convert thickness from ms to m.

ID	Acoustic signature		Bounding reflectors	Geometry/Thickness	Distribution	Interpretation
AF1	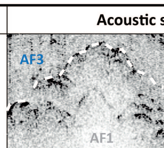	Semi-transparent, weak, chaotic internal reflections that disappear with depth	Lower: not detected Upper: hummocky, variably strong, discontinuous	Thickness: >10 ms (≈7.5 m)	As acoustic basement in entire fjord	Bedrock
AF2	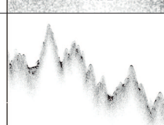	Semi-transparent; chaotic internal reflections that weaken with depth	Lower: discontinuous, hummocky, variably strong Upper: strong, mostly continuous, hummocky in inner fjord basin	Thickness: 1-20 ms (≈1.75-15 m)	Overlying AF1 in most of the fjord, also occurs as S2 in both Ymerbukta and Trygghamna	Glacial till
AF3	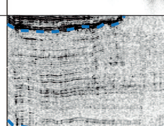	Variable from massive and (semi-)transparent to acoustically stratified	Lower: variably strong, (dis-)continuous Upper: strong, opaque, mostly continuous	Conformable geometry Thickness: <24 ms (≈18 m)	Common in basins, overlies AF1 or AF2; also occurs in Ymerbukta and Trygghamna as S4a	Gacimarine mud from suspension settling; occasionally coincide with mass flows
AF4	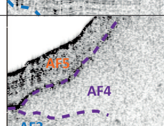	Semi-transparent, weak, massive internal reflections	Lower: weak, mostly continuous Upper: continuous, variably strong	Occurs as lenses or wedge-shaped deposits that laterally pinch out Thickness: 2-22 ms (≈1.5-16.5 m)	Central fjord, common at the foot of slopes, often appears intercalated into AF3	Turbidity currents or alternative mass-flow deposits (MTDs)
AF5	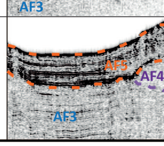	Acoustically stratified, parallel, opaque internal reflections	Lower: continuous, variably strong Upper: seabed	Conformable geometry, overlies AF4 Thickness: <6 ms (≈4.5 m)	Inner fjord, also occurs in Ymerbukta and Trygghamna as S6	Late Holocene glacimarine or hemipelagic mud; occasionally coincides with MTDs

appearance varies from internally massive and semi-transparent to acoustically stratified (Table 2, Fig. 5c). It has a strong and opaque, relatively continuous upper boundary and is especially common in bathymetric basins (Fig. 5b, c). AF4 is acoustically (semi-)transparent with weak internal reflections of a massive nature that disappear in places (Table 2, Fig. 5c). The facies occurs as lenses or wedge-shaped deposits, often intercalated into AF3 (Fig. 5) and commonly appears at the foot of slopes where it pinches out with increasing distance from the slope (Fig. 5c, d). AF5 is the stratigraphically uppermost facies in Magdalenefjoden, and thus the inferred youngest. It is bounded by the seabed on top and appears acoustically stratified (Fig. 5c). AF5 is present in the inner fjord, i.e. ice-proximal areas, and conformably overlies AF4 (Fig. 5).

Interpretation

AF1 is interpreted as the acoustic basement in Magdalenefjorden, the acoustic appearance of which suggests that AF1 represents either glacial till or bedrock (cf. Forwick et al., 2010; Forwick & Vorren, 2012; Kempf et al., 2013; Roy et al., 2014). Its stratigraphic position, the hummocky upper boundary, and the outcropping bedrock visible on the swath-bathymetric data (Fig. 5) all indicate that the acoustic basement in Magdalenefjorden comprises bedrock.

AF2 is acoustically similar to AF1 and to acoustic facies from other Spitsbergen fjords, including Unit S2 in Ymerbukta and Trygghamna (cf. Forwick & Vorren, 2011, 2012; Kempf et al., 2013) and is thus interpreted as glacial till. This would imply a diamictic composition for the sediments of AF2, which is supported by the massive acoustic appearance and weakening internal reflections with depth (cf. Stewart & Stoker, 1990; Forwick & Vorren, 2012). In innermost Magdalenefjorden AF2 crops out at the seafloor and its very hummocky appearance here correlates with the occurrence of the recessional moraines (Fig. 5), also supporting an interpretation as glacial till.

The (semi-)transparent, partially stratified acoustic signature of AF3 supports an interpretation as glacimarine sediments derived from suspension settling from meltwater plumes (e.g. Plassen et al., 2004; Kempf et al., 2013; Streuff et al., 2015). Where the facies appears stratified, regular changes in lithology or density are implied, which could indicate a glacier-proximal depositional environment (cf. Syvitski, 1989; Forwick & Vorren, 2012), possibly with the occurrence of turbidity currents or other gravitational mass flows (e.g. Sexton et al., 1992; Forwick & Vorren, 2012; Streuff et al., 2017). In places the latter is also indicated by the localised appearance of AF4 (see below). AF3 is similar to S4a in Ymerbukta and Trygghamna (cf. Forwick & Vorren, 2011, 2012).

AF4 is interpreted as mass-flow deposits. This is supported by the lenticular appearance, the internally massive semi-transparent acoustic signature, and its similarity with such deposits in other areas around Svalbard (e.g Plassen et al., 2004; Forwick & Vorren, 2007; Hogan et al., 2010; Forwick & Vorren, 2012; Kempf et al., 2013; Streuff et al., 2015).

AF5 is interpreted as late Holocene glacimarine or hemipelagic sediments delivered into the fjord by meltwater streams (cf. S6 in Ymerbukta and Trygghamna, AF6 in Lomfjorden; Forwick & Vorren, 2011; Streuff et al., 2017). Similar to S5 and S6, the internal reflections could indicate periods of increased iceberg rafting (cf. Forwick & Vorren, 2009, 2011). However, our lithological data suggest that the stratification is probably the result of repeated changes in grain size and possibly mass flow activity (see section 4.3 below).

4.3. Lithostratigraphy

4.3.1. Lithofacies

Description

Based on the sedimentary evidence, we define a total of four lithofacies, LF1–

Table 3: Lithofacies in Magdalenefjorden with examples of the facies in core logs and on x-radiographs. For physical properties MS = Magnetic Susceptibility, WC = Water Content, and ρ = wet-bulk density as measured with the MSCL.

Litho-facies	Log (Clay, Silt, Sand)	X-ray	Material	Physical parameters	Distribution	Interpretation
LF1	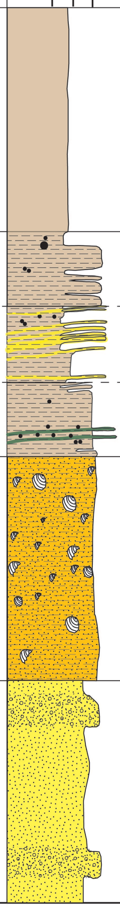	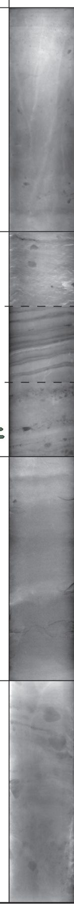	massive, greyish brown, no internal structures, very few clasts, occasionally bioturbated	2.5Y 5/2 - 4/2 >90% clay + silt MS ≈ 20 WC = 25-30% ρ ≈ 1.8-2.1 g/cm³	Upper 25 cm of GC01 and GC03 (Fig. 6)	Distal glacimarine mud settling from suspension in glacial meltwater plumes and the water column
LF2a			weakly stratified, partially bioturbated; occasional clasts and load structures	2.5Y 5/2 - 4/2 >98% clay + silt MS ≈ 10-20 WC = 20-35% ρ ≈ 1.9-2.25 g/cm³	GC01, GC03 (Fig. 6)	Distal glacimarine mud settling from suspension in meltwater
LF2b			stratified, couplets of sharp-bounded coarse and fine layers, occasionally with LF4			Proximal glacimarine mud, deposition from suspension probably seasonally controlled
LF2c			(diffusely) stratified mud with thin diamict layers, gradual contacts			Glacimarine mud with IRD, deriving from suspension and icebergs/sea ice
LF3			diffusely laminated, dark grey at surface, black in sub-surface, strong smell of H2S, commonly shell fragments and bivalves	5Y 4/1 5Y 2.5/1 40-80% clay + silt MS ≈ 5-10 WC = 20-35% ρ ≈ > 2 g/cm³	GC06 (Fig. 6)	Distal glacimarine mud settling from suspension in glacial meltwater plumes from different sources. High organic content likely cause of seasonal control on biological productivity
LF4			massive sandy mud, occurs as thin beds or thick strata, strong smell of H2S, black sub-surface, few shell fragments, sharp contacts	2.5Y 4/2 -5/2 5Y 2.5/1 60-80% clay + silt MS ≈ 15-30 WC = <25% ρ ≈ 2-2.5 g/cm³	GC03, GC06, GC09 (Fig. 6)	Glacier outwash or sediment remobilised during gravitational mass flows

LF4 in Magdalenefjorden (Fig. 6). Their characteristics are summarised in Table 3.

LF1 contains massive mud with > 90% clay and silt and only occurs in the top 25 cm of GC01 and GC03 (Table 3). It shows no internal structures and very few clasts (Fig. 6). The water content (Table 3) is a minimum value, as both cores were split in 2009, and it is likely that the sediments dried out to some extent since then.

LF2 contains finely laminated to stratified mud with occasional clasts and occurs in GC01 and GC03. Like in LF1, the mud is generally very fine (Table 3, Fig. 6). Black mottles appear throughout the facies. We define laminae as thinner than 1 cm (but usually up to only 2 mm in Magdalenefjorden), and strata, which are between 1 and 5 cm thick. The greyscale changes in the x-radiographs suggest that the stratified nature of the sediments is likely caused by differences in grain size or density (Fig. 6c, f). The latter is supported by the strong oscillations in bulk density (Fig. 6). The water content, as for LF1, is a minimum value. We distinguish three subfacies of LF2: LF2a, LF2b, and LF2c. LF2a contains weakly or diffusely stratified, partially bioturbated mud where no significant changes in grain size occur between individual layers (Fig. 6f). Occasional clasts within the facies may be accompanied by load structures. In LF2b the stratification is more pronounced and defined by couplets of sharp-bounded coarser and finer layers of variable thickness (Fig. 6f). Bioturbation traces are absent. Layers may be inclined with undulating contacts and contain the fine massive sand of LF4 (see below) in places. LF2c contains (diffusely) stratified mud, which appears intercalated with thin layers of a matrix-supported diamict (Fig. 6c, f). The boundaries between mud and diamict are gradual and lack load structures (Fig. 6f).

LF3 only occurs in GC06 and contains diffusely laminated mud with a relatively high silt and sand content (Table 3, Fig. 6). The sediments are dark grey at the surface, and black in the subsurface, and emit a strong smell of H_2S. Shell fragments and entirely preserved bivalves are common and may occur in concentrated layers or scattered throughout (Fig. 6). The slightly coarser nature of LF3 is reflected in the grain size distribution, which commonly shows 40–80% of the sediments to be finer than 63 μm (Table 3, Fig. 6). Although the water content of 20–35% is similar to the fine-grained mud of LF2a, it is important to note that GC06 was one of the two cores split in 2016, its water content is thus regarded as more reliable, and the water content of LF2a may consequentially be higher than measured.

LF4 occurs as thin beds or as thick strata and has a massive, unsorted appearance. It contains fine sand with small, but variable amounts of mud and sparsely scattered clasts and shell fragments (Table 3). During core splitting a strong H_2S odour occurred and the sediments' subsurface is characterised by a black colour. Boundaries to other lithofacies are often sharp (Fig. 6). GC09 is only composed of LF4 (Fig. 6b).

Interpretation

LF1 is similar to massive muds observed in other glacimarine settings and is interpreted as mud settling from suspension in meltwater plumes or the water column. The massive internal structure and the presence of occasional bioturbation structures indicate ice-distal conditions during the accumulation of LF1 (cf. e.g. Elverhøi et al., 1983; Forwick & Vorren, 2009; Baeten et al., 2010).

The stratified muds of LF2 are similar to sediments documented from other fjords in Spitsbergen and are accordingly interpreted as glacimarine mud deposited in a relatively calm, meltwater-dominated depositional environment (cf. e.g. Elverhøi et al., 1983; Plassen et al., 2004; Forwick et al., 2010; Streuff et al., 2015). Laminated or stratified glacimarine muds commonly occur in Arctic fjords, where they are usually associated with an interplay of depositional processes or sedimentation from multiple sources (cf. e.g. Elverhøi et al., 1980; Ó Cofaigh & Dowdeswell, 2001; Forwick & Vorren, 2009; Streuff, 2013). Stratification and lamination of LF2 and its subfacies in Magdalenefjorden could thus be a consequence of (1) multiple glaciers delivering sediments to the source, (2) tidally controlled release of the suspension load carried in the meltwater plumes,

(3) diurnal or seasonal variation in meltwater flux and thus depositional energy, and (4) an interplay between suspension settling from meltwater plumes and repeated gravity flows (e.g. Elverhøi et al., 1983; Mackiewicz et al., 1984; Cowan & Powell, 1990; Ó Cofaigh & Dowdeswell, 2001; Gilbert et al., 2002). This is further discussed in section 5.2 below.

LF3 is similar to LF2a with the main differences being darker sediments and coarser grains in LF3. Above, we suggested a number of processes that could lead to the stratified appearance of glacimarine mud for the formation of LF2, and infer that similar processes deposited LF3 (see also section 5.2 below). Black mottles and the smell of H_2S are suggested to reflect monosulphid layers, formed from seasonal variations in biological productivity (e.g. Elverhøi et al., 1980, 1983).

The unsorted and massive appearance of LF4 as well as the coarser grain sizes are interpreted as the result of sediment accumulation in a high-energy depositional environment, i.e. from gravity flows. Where LF4 occurs as thin beds or lenses, these flows were probably of relatively small magnitude and could represent turbidite deposits in a glacier-proximal environment (cf. e.g. Gilbert, 1982; Gilbert et al., 1993). Larger packages of LF4, such as at the top of GC06, may accordingly result from more extensive mass-transport deposits, which commonly occur in Svalbard fjords, especially along the fjord walls (e.g. Forwick & Vorren, 2007, 2012; Streuff et al., 2017, this study).

4.3.2. Radiocarbon dates and sediment accumulation rates

Six radiocarbon dates were obtained from foraminifera and molluscs from GC01 and GC06 in Magdalenefjorden. The dates are displayed in Table 4 and Figure 7.

The results from the AMS dating show that the sediments in GC01 reflect recent deposition, with a basal date of ~505 cal a BP, an age of ~319 cal a BP

Table 4: Radiocarbon dates from this study, calibrated using a ΔR of 61 ± 70 (Mangerud, 1972). Note that the reported age for Beta–434937 indicates an age of post 1950 AD and is therefore given in percent modern carbon (pMC) of the modern reference standard.

Core ID	Depth [cm]	Lab Code	Sample	Reported age [^{14}C a BP]	Median [cal a BP]	2σ [cal a BP]
GC01	25	Beta–447123	Foraminifera	660 ± 30	228	0–20; 49–410
GC01	254	Beta–447124	Foraminifera	730 ± 30	319	131-472
GC01	359-363	Beta–448203	Foraminifera	950 ± 30	505	360-640
GC06	3.5	Beta–434937	Bivalve	106.2 pMC ± 0.3	NA	∼0–60
GC06	12	Beta–434938	Single valve	560 ± 30	132	0–262
GC06	35	Beta–434939	Fragmented bivalve	550 ± 30	124	0–257

for a sediment depth of 254 cm, and an age of ∼228 cal a BP at a sediment depth of 25 cm (Table 4, Fig. 7). As all dates stem from around 6 mg of generally well-preserved benthic foraminifera we consider the foraminifera in GC01 to reflect in-situ conditions and infer that the obtained ages are reliable. Assuming a linear rate of sediment accumulation, the dates from GC01 suggest that LF2a in the lower parts of the core accumulated at a rate of ∼0.49 cm a^{-1}, whereas LF2b, between 254 and ∼50 cm sediment depth, accumulated at a rate around 3.3 cm a^{-1}. LF1 in the topmost 25 cm of the core was deposited at a sediment accumulation rate (SAR) of 0.04 cm a^{-1} (Fig. 7). The relatively high SAR in the central parts of the core suggests that an interpretation of LF2b as ice-proximal sediments is reasonable (cf. e.g. Elverhøi et al., 1980, 1983). Similarly, the lower SAR of the topmost 25 cm supports a distal glacimarine environment. The sediments in GC06 are younger than those in GC01, as the AMS dating shows ages of ∼124 cal a BP for a sediment depth of 35 cm, ∼132 cal a BP for a sediment depth of 12 cm, and an age of <60 years for the sediments around 3.5 cm core depth. The age reversal between the two lowermost dates in GC06 may indicate that the single valve at 12 cm was reworked, but considering the very young ages of the sediments at both depths, the large error range may easily account for the older age at 12 cm. Furthermore, the weakly stratified nature of LF3 and the good preservation of the shells sampled suggest that sediment reworking is unlikely in this part of the core. The two ages at 12 and 35 cm could thus suggest that the shells were deposited simultaneously and that LF3 in GC06 accumulated quasi-instantaneously. However, as there is some evidence of bioturbation in the core, it is also possible that the age reversal at 12 cm was caused by post-depositional upward migration of an older shell into younger sediments. If this were the case, LF3 was deposited at a SAR of 0.25–0.49 cm a^{-1} in GC06, indicating that this lithofacies was probably deposited in a similar environment to LF2a.

5. Discussion

5.1. Landform assemblages in Ymerbukta, Trygghamna and Magdalenefjorden

The landforms described from Ymerbukta, Trygghamna, and Magdalenefjorden include (1) bedrock highs, (2) overridden recessional moraines, (3) glacial lineations, (4) terminal moraines, (5) deposits from gravitational mass flows, (6) unmodified recessional moraines, (7) De Geer moraines, and (8) pockmarks. While there is some variability in the landforms observed in the outer fjord basins, the landform assemblages in the ice-proximal basins adjacent to the present glacier fronts are remarkably similar. In Ymerbukta and Trygghamna the more distal fjord basins are characterised by a relatively smooth seafloor with pockmarks and debris flow deposits as the only landforms. In Magdalenefjorden, pockmarks and mass flow deposits are absent and bedrock highs and partially buried recessional moraines are the only features observed. The smooth seafloor in all three fjords suggests some degree of sediment draping, possibly masking underlying landforms (cf. Ottesen & Dowdeswell, 2009), which is confirmed by the thick sedimentary sequences observed on the sub-bottom profiler data (Forwick & Vorren, 2011, 2012, this study). The presence or absence of debris flows could be related to local differences in sediment availability, accumulation rates, exposure to earthquakes, and/or the presence or absence of gaseous fluids beneath the seafloor (cf. e.g. Hovland & Judd, 1988; Forwick et al., 2009; Forwick & Vorren, 2012).

Based on the presence of the landforms in the inner fjord basins and their relationship with each other, we define three landform assemblages, one for each fjord. All assemblages are named after their inferred source glacier. The Esmarkbreen Assemblage occurs in Ymerbukta and comprises overridden recessional moraines, glacial lineations, a terminal moraine and associated debris lobes on its distal flank, and a number of De Geer moraines. The Kjerulfbreen-Harrietbreen Assemblage in Trygghamna is made up of a terminal moraine and an associated debris lobe, three recessional moraines, and a sequence of De Geer moraines. The three recessional moraines and the De Geer moraines in inner Magdalenefjorden form the Waggonwaybreen Assemblage. Their formation is discussed in section 5.3 below.

5.2. Sedimentary environments

From the lithological data in Magdalenefjorden, we identify three main sedimentary processes in the fjord: (1) suspension settling of fine-grained glacimarine mud from glacial meltwater, (2) delivery of clasts to the fjords as ice-rafted debris melting out from icebergs and sea ice, and (3) abundant gravitational mass flows reworking the accumulated sediments. The first process, i.e. the rain-out of suspension load from meltwater, is the most dominant process in Magdalenefjorden, where the seafloor is covered by a relatively thick sequence of glacimarine muds. These muds are massive at the top of GC01 and GC03 (LF1), where they overlie the (diffusely) stratified mud of LF2. While the depositional process is the same for both lithofacies, the different internal structure indicates slight changes in the depositional environment. Massive mud as recorded in LF1 could reflect more distal conditions, in which there is insufficient energy to transport coarser grains to the core sites and high-energy gravitational processes are rare. Ice-distal conditions and thus lower energy during the accumulation of LF1 are further supported by the low SAR of 0.04 cm a^{-1} and the scattered bioturbation traces (cf. e.g. Elverhøi et al., 1980; Lønne & Mangerud, 1991; Sexton et al., 1992; Baeten et al., 2010). Similar conditions are inferred for the diffusely stratified sediments of LF2a. In contrast, the more pronounced lamination or stratification characteristic of LF2b is considered to be consistent with a more glacier-proximal setting (e.g. Elverhøi et al., 1983; Ó Cofaigh & Dowdeswell, 2001; Forwick & Vorren, 2009), where individual strata were formed due to regular variations in depositional energy. Thinner, more rhythmic laminae, for instance, probably derive from semi-regular changes in meltwater supply or suspension release from the meltwater plumes, which could be tidally or seasonally controlled (e.g. Elverhøi et al., 1980; Mackiewicz et al., 1984; Cowan et al., 1997; Ó Cofaigh & Dowdeswell, 2001). Given the sedimentation rate of 3.7 cm a^{-1} in GC01 we can infer that two such couplets occur per year (in 4 cm of sediment), providing evidence that some of these laminations are indeed seasonally controlled. The abundance of black mottles in LF2 supports this, as it is possibly related to seasonal variations in biological productivity, where black layers reflect diatom blooms in spring (Elverhøi et al., 1980, 1983). Where the lamination or stratification is more irregular, and sandy beds occur, the deposition of glacimarine mud from meltwater is probably influenced by punctuated single events, such as turbidity currents. This is supported by the sharp-based, sometimes undulating boundaries of the sand layers and their downward inclination (see Fig. 6f), which are common features of turbidite deposits from glacier-proximal environments (e.g. Kuenen, 1948; Gilbert, 1982; Powell & Molnia, 1989; Gilbert et al., 1993). The relatively high SAR around 3 cm a^{-1} and the absence of bioturbation traces within this facies further support a glacier-proximal origin for LF2a. The clasts scattered throughout the glacimarine muds in Magdalenefjorden likely represent IRD and therefore imply that sedimentation from icebergs and sea ice is another process influencing the depositional environment in the fjord. However, the relatively low number of clasts emphasises the importance of sedimentation from meltwater, which partly masks the input from IRD. Individual clasts in lithofacies LF2a are probably dropstones, as indicated by the occasional presence of load structures. The rare diamictic and clast-rich layers embedded into the weakly stratified mud of LF2c on the other hand probably originate from concentrated melting events, either related to iceberg turnover or to the meltout of IRD from shore-fast sea ice and entrapped icebergs during summer, while the surrounding mud was deposited during winter when IRD supply was suppressed (cf. Syvitski et al., 1996; Jennings & Weiner, 1996; Dowdeswell et al., 2000). Considering the nearly stratified appearance of the diamict layers, the gradual, quasi-horizontal contacts (see Fig. 6f), and the absence of load clasts, seasonally-controlled sedimentation appears to be more likely than iceberg dumping.

Similar to LF2a, LF3 is interpreted as relatively ice-distal glacimarine mud. The colour difference between the two facies could indicate a different meltwater source, i.e. variable sediment provenance (cf. Forwick & Vorren, 2009; Forwick et al., 2010), an assumption that seems reasonable when considering the location of the core sites. GC01 and GC03, which predominantly contain LF1, are located in the inner and central fjord and are thus likely influenced by meltwater supplied by the four glaciers at the head of the fjord, Buchanbreen, Waggonwaybreen, Miethebreen, and Brokebreen. The core site of GC06 in the outer fjord, on the other hand, may additionally be influenced by sediment supply from Gullybreen, Adambreen, and Skarpeggbreen (see Fig. 2). The strong smell of H_2S and the generally darker sediment colour is probably related to a relatively high organic content, which, again, could contribute to the diffuse stratification in the form of annual monosulphid layers formed by spring algal bloom (Elverhøi et al., 1980, 1983).

The massive sand intermixed with glacimarine mud in LF4 is interpreted as a product of glacier outwash, especially in the inner fjord, or of larger mass-transport events. The latter is more likely, as the frequent occurrence of such events in all fjords is also attested to by the sedimentary lobes visible on the bathymetric data and by the appearance of the lenticular bodies of AF4 and S4a, which were at least partially interpreted as gravity-flow deposits (Forwick & Vorren, 2011, this study). The fact that GC09 and GC06 only contain LF3 and LF4 shows that these core sites are located in a relatively high-energy depositional environment, where such events are frequent, which is a logical consequence of their relatively ice-proximal location.

Although we have no lithological evidence from Ymerbukta and Trygghamna, we suggest that similar sedimentary processes to those in Magdaleneforden also operate in the two Isfjorden tributaries. This is based on the sub-bottom profiler data, showing that sedimentary facies in the three fjords are very similar, and that sedimentation is controlled by glacial meltwater, occasional icebergs, and occasional to frequent gravitational mass flows (Forwick & Vorren, 2011, 2012, this study). This corroborates the findings of previous studies, which showed that the sedimentary processes in front of tidewater glaciers are generally similar, and that it is more the magnitude and the different factors controlling sedimentation rather than the individual processes themselves that vary with climate and locality (e.g. Elverhøi et al., 1983; Cowan et al., 1999; Ó Cofaigh & Dowdeswell, 2001; Ó Cofaigh et al., 2001; Gilbert et al., 2002; Streuff et al., 2017).

5.3. Evolution of the sediment-landform assemblages and associated glacier dynamics

From the different landform assemblages observed in the three fjords, we infer regionally variable glacier dynamics. In Ymerbukta, the Esmarkbreen Assemblage is consistent with submarine landform assemblages deposited from glacier surges (e.g. Solheim & Pfirman, 1985; Ottesen et al., 2008; Flink et al., 2015; Streuff et al., 2015), not least because the crevasse-squeeze component in the De Geer moraines may be indicative of surge activity (cf. e.g. Sharp, 1985; Ottesen & Dowdeswell, 2006; Farnsworth et al., 2016). The presence of overridden moraines indicates that Esmarkbreen experienced at least one re-advance after deglaciation. Given that Esmarkbreen was not part of the original surge-type glacier inventory put forward by Hagen et al. in 1993, but was recently identified as surge-type based on the presence of crevasse-squeeze ridges observed in the glacier's terrestrial foreland (Farnsworth et al., 2016), Esmarkbreen probably only surged recently (2014; Allaart et al., 2015), suggesting that most of the landforms in the Ymerbukta assemblage are relatively young. The exceptions are the overridden moraines, that must have formed prior to the surge and thus provide evidence for episodic ice retreat during deglaciation or after a LIA advance of Esmarkbreen. A later re-advance, likely related to a surge of Esmarkbreen, formed the glacial lineations during the active phase of rapid advance, the terminal moraine and the associated debris lobe during the transition from active to passive phase, and a sequence of De Geer moraines during subsequent episodic retreat. If we assume that the De Geer moraines were formed each year during winter as suggested for other Spitsbergen fjords (e.g. Ottesen & Dowdeswell, 2006; Ottesen et al., 2008) the total number of such moraines in Ymerbukta should indicate that Esmarkbreen surged around 50 years ago. However, given the crevasse-squeeze component of some of these ridges, the fact that Esmarkbreen did not show surge-like behaviour until ∼2010 (Heidi Sevestre, pers. comm.), and the comparatively small number of De Geer moraines in Trygghamna and Magdalenefjorden (see below), we suggest that the moraines form much less regularly than previously thought and may not necessarily be related to winter re-advances.

Glacier dynamics such as those suggested here for Esmarkbreen have been documented for a large number of Spitsbergen surge-type glaciers (cf. Solheim & Pfirman, 1985; Solheim, 1991; Boulton et al., 1996; Christoffersen et al., 2005; Ottesen et al., 2008; Kristensen et al., 2009; Flink et al., 2015; Streuff et al., 2015), supporting the hypothesis that Esmarkbreen is indeed a surging glacier (Farnsworth et al., 2016). The sub-bottom profiler data from the fjord shows that sedimentation was largely similar throughout the Holocene with mud settling from glacial meltwater, IRD melting out from icebergs and or sea ice, and occasional mass transport events reworking the accumulated deposits (Forwick & Vorren, 2009, 2011).

In Trygghamna we identified 29 De Geer moraines and a large debris lobe on the flank of the outermost moraine (see Figs. 3, 4d) as part of the Kjerulfbreen-Harrietbreen Assemblage. This outermost moraine could represent a terminal moraine marking the Holocene maximum ice extent in the fjord. Despite the similarities in landforms between Trygghamna and Ymerbukta, and although both Kjerulfbreen and Harrietbreen at the head of Trygghamna have recently been identified as surge-type glaciers (Farnsworth et al., 2016), we hesitate to ascribe a definitive surge origin to the submarine landforms in Trygghamna.

This is mainly because the absence of overridden moraines indicates only one Holocene re-advance of the glaciers in the fjord, which could also be related to the LIA cooling rather than a surge (cf. e.g. Plassen et al., 2004; Ottesen & Dowdeswell, 2006; Forwick et al., 2010), and because the absence of glacial lineations suggests relatively slow ice flow (cf. King et al., 2009), which is atypical for the active phase of a surging glacier (e.g. Meier & Post, 1969; Raymond, 1987; Sharp, 1988; Benn & Evans, 2010). The landform assemblage in Trygghamna could thus be a product of ice retreat, either during deglaciation or after the LIA, with the outermost moraine indicative of a prolonged period of still-stand related to either (i) shoaling waters and accordingly slowed glacier retreat (e.g. Oerlemans & Nick, 2006; Benn et al., 2007; Kehrl et al., 2011), or (ii) the transition between ice advance and ice retreat during the LIA. Nevertheless, if crevasse-squeeze ridges are indeed surge-diagnostic landforms, their presence in the terrestrial forelands of both glaciers (Farnsworth et al., 2016), and the variable orientations of some of the submarine De Geer moraines should suggest that the entire landform assemblage formed from a glacier surge. Based on the absence of overridden moraines and glacial lineations, we suggest that formation of the terminal moraine and the associated debris lobe in Trygghamna occurred as a result of a re-advance of Harrietbreen and Kjerulfbreen during the LIA cooling (cf. Ottesen & Dowdeswell, 2006), but note that glacier advance and subsequent landform formation could have occurred from both glacier surging or LIA advances. Similar conclusions have also been drawn for the adjacent Borebukta and Yoldiabukta (Ottesen & Dowdeswell, 2006).

The debris lobes and pockmarks in the outer parts of both Ymerbukta and Trygghamna must have formed during the Holocene after the fjord was ice-free, as a grounded glacier would have prevented the deposition of large mass-transport deposits and the escaping of fluids from the seafloor (cf. Forwick et al., 2009; Forwick & Vorren, 2012).

Glacial lineations in Isfjorden are transverse to the direction of inferred ice flow through Ymerbukta and Trygghamna and are thus likely the product of ice streaming east to west through the fjord during the LGM (cf. e.g. Landvik et al., 1998; Ottesen et al., 2005). The ice-marginal wedge provides evidence for an extended period of still-stand during overall glacier retreat.

In Magdalenefjorden, the presence of a deep bathymetric basin in the central fjord complicates the reconstruction of the local ice dynamics, as it is difficult to ascertain whether a lack of glacial landforms within the central parts of this basin is related to (i) partial ungrounding of the retreating ice margin during deglaciation, or (ii) post-glacial sediment masking. The De Geer moraines in the fjord could thus have formed during episodic ice retreat related to either deglaciation or a LIA re-advance of the local glaciers. As the moraines or parts thereof occur within the entire fjord and along the steep side walls of the bathymetric basin, it is likely that at least the moraines in the outer fjord, and possibly those within the basin, were deposited during deglaciation when ice retreated from its maximum position at the continental shelf edge (cf. Ottesen & Dowdeswell, 2009). In the inner fjord, the moraines could also be a product of Holocene glacier re-advance and subsequent retreat. Indeed, the most distal of the De Geer moraines here is slightly larger than the rest and was previously interpreted as a terminal moraine marking the maximum ice extent of Waggonwaybreen during the LIA (Ottesen & Dowdeswell, 2009). This interpretation is supported by our lithological evidence and sub-bottom profiler data which show the presence of a small and localised debris flow down the moraine's distal flank. We note, that in this instance the assumption of annual formation for the De Geer moraines would also be unreasonable, as the total number of 37 would suggest that Waggonwaybreen reached its LIA maximum less than 40 years ago.

From the lithological data in Madalenefjorden we summarise the following chronology for the sediments in the fjord: LD2a is the oldest recovered facies in the cores and was deposited during relatively ice-distal conditions. Based also on the AMS date of around 500 cal a BP, it is likely that this subfacies was deposited during glacier retreat during deglaciation, probably before the LIA. The fact that GC03 mostly contains LF2a shows that the sedimentary processes at this core site were largely the same throughout the Holocene. In GC01 LF2a is overlain by LF2b, which was interpreted as proximal glacimarine sediment. The stratification, the high SAR and the accumulation of this facies relatively soon after ∼320 cal a BP could suggest that Waggonwaybreen re-advanced in response to the LIA cooling. The increasingly more diffuse stratification up-core of GC01 and the re-appearance of LF2a before ∼230 cal a BP implies that retreat after the LIA advance was already underway at this point. The ice-distal sediments of LF1 at the top of both GC01 and GC03 indicate that the glacier front had retreated relatively far back from the core sites by ∼230 cal a BP.

Lithofacies LF3 reflects the contemporary sedimentary environment at the core site of GC06, where the input from many different sources maintains a high sediment accumulation rate and causes occasional small changes in the depositional environment. Since LF4 was interpreted as deposits from gravitational mass-flow events, this lithofacies is chronologically independent, as such events can occur at any time. Nevertheless, where the facies occurs as thin beds in the mud of LF2b in GC01, the deposition of LF4 was likely related to the possible re-advance of Waggonwaybreen during the LIA.

6. Conclusions

Swath-bathymetric data from three fjords reveal the landform assemblages in front of several Spitsbergen tidewater glaciers. While the main processes forming the landforms are somewhat similar, individual glacier dynamics control the occurrence of different types of landforms. In Ymerbukta, one or more surges of Esmarkbreen are indicated by the presence of overridden moraines and glacial lineations, formed during retreat followed by relatively fast glacier re-advance. A terminal moraine and associated debris lobe mark the maximum extent of the glacier during the Holocene, and the occurrence of numerous De Geer moraines provides evidence for subsequent step-wise retreat. Processes of crevasse-squeezing are implied by the variable orientation and occasional cross-cutting of these moraines. In the adjacent Trygghamna a terminal moraine and debris lobe were probably formed as a result of a LIA re-advance of the two glaciers Kjerulfbreen and Harrietbreen at the head of the fjord, after which retreat was similarly episodic as in Ymerbukta.

In Magdalenefjorden in northeast Spitsbergen a slightly larger moraine at the edge of the innermost basin is probably related to a re-advance of Waggonwaybreen in response to the LIA around 300 cal a BP. The characteristic debris lobe often associated with the distal flank of such terminal moraines in Svalbard fjords appears to be unusually small in Magdalenefjorden, suggesting that the glacier front halted there for only a short period of time, or that sediment availability was restricted. Retreat, as indicated by numerous De Geer moraines, was also episodic. Our data interpretation indicates, that contrary to previous assumptions, De Geer moraines can form much less frequently than once a year. The transition from distal to proximal to distal glacimarine mud in one of the gravity cores from Magdalenefjorden reflects a sequence of glacier retreat, likely related to deglaciation after the LGM, glacier re-advance probably related to the LIA cooling, and subsequent retreat of the glacier front. Distal glacimarine muds are massive to weakly stratified with occasional evidence of bioturbation, and were deposited at relatively low rates of 0.04–0.49 cm a^{-1}. Ice-proximal glacimarine muds are distinctly laminated or stratified and contain couplets of one coarser and one finer layer, which probably derive from seasonally controlled suspension rainout from meltwater plumes. The occurrence of turbidity currents is indicated by the presence of several thin sandy layers in the glacimarine mud. The proximal stratified muds accumulated at a rate of around 3 cm a^{-1}.

The lithofacies observed in the gravity cores reveal that suspension settling from meltwater plumes and the water column is the dominant sedimentary process in Magdalenefjorden, with very occasional input of IRD from icebergs and sea ice. These sediments are reworked as a consequence of turbidity currents close to the glacier fronts and of other mass-flow events such as slides and slumps down steep submarine slopes. Our data interpretation suggests that components of landform assemblages as well as sedimentary processes in glacimarine environments are largely similar and that small variations across wider areas are controlled by localised changes in glacier hydrology, thermal regime, sediment availability, bathymetry and air/ocean temperatures, rather than different geographic location and climate.

Acknowledgments

This work, as part of the GLANAM project "Glaciated North Atlantic Margins", was funded by the People Programme (Marie Curie Actions) of the European Union's Seventh Framework Programme FP7/2007-2013/ under REA grant agreement no. 317217.

We thank the captain and crew of *R/V Helmer Hanssen* (previously *Jan*

Mayen) for their help with data acquisition. Constructive feedback from Brian Todd and an anonymous reviewer was highly appreciated and helped to further improve this manuscript.

Allaart, L., Håkansson, L., & Noormets, R. (2015). Field guide GLANAM 3rd workshop and field excursion in Isfjorden, Svalbard. URL: http://www.glanam.org/wp-content/uploads/2017/03/Fieldguide_3AnnualMeeting_Ymerbukta_2015.pdf.

Baeten, N., Forwick, M., Vogt, C., & Vorren, T. (2010). Late Weichselian and Holocene sedimentary environments and glacial activity in Billefjorden, Svalbard. *Geological Society, London, Special Publications*, *344*, 207–23. doi:10.1144/SP344.15.

Batchelor, C., & Dowdeswell, J. (2015). Ice-sheet grounding-zone wedges (GZWs) on high-latitude continental margins. *Marine Geology*, *363*, 65–92. doi:10.1016/j.margeo.2015.02.001.

Benn, D., & Evans, D. (2010). *Glaciers and Glaciation*. (2nd ed.). Hodder Education.

Benn, D., Warren, C., & Mottram, R. (2007). Calving processes and the dynamics of calving glaciers. *Earth-Science Reviews*, *82*, 143–79. doi:10.1016/j.earscirev.2007.02.002.

Błaszczyk, M., Jania, J. A., & Hagen, J. O. (2009). Tidewater glaciers of Svalbard: Recent changes and estimates of calving fluxes. *Polish Polar Research*, *30*, 85–142.

Blatter, H., & Hutter, K. (1991). Polythermal conditions in Arctic glaciers. *Journal of Glaciology*, *37*, 261–9. doi:10.3198/1991JoG37-126-261-269.

Boulton, G. (1986). Push-moraines and glacier-contact fans in marine and terrestrial environments. *Sedimentology*, *33*, 667–98. doi:10.1111/j.1365-3091.1986.tb01969.x.

Boulton, G., Van Der Meer, J., Hart, J., Beets, D., Ruegg, G., Van Der Wateren, F., & Jarvis, J. (1996). Till and moraine emplacement in a deforming bed surge – an example from a marine environment. *Quaternary Science Reviews*, *15*, 961–87. doi:10.1016/0277-3791(95)00091-7.

Christoffersen, P., Piotrowski, J. A., & Larsen, N. K. (2005). Basal processes beneath an Arctic glacier and their geomorphic imprint after a surge, Elisebreen, Svalbard. *Quaternary Research*, *64*, 125–37. doi:10.1016/j.yqres.2005.05.009.

Cowan, E., Cai, J., Powell, R., Clark, J., & Pitcher, J. (1997). Temperate glacimarine varves: an example from Disenchantment Bay, southern Alaska. *Journal of Sedimentary Research*, *67*, 536–49.

Cowan, E., & Powell, R. (1990). Suspended sediment transport and deposition of cyclically interlaminated sediment in a temperate glacial fjord, Alaska, USA. *Geological Society, London, Special Publications*, *53*, 75–89. doi:10.1144/GSL.SP.1990.053.01.04.

Cowan, E. A., Seramur, K. C., Cai, J., & Powell, R. D. (1999). Cyclic sedimentation produced by fluctuations in meltwater discharge, tides and marine productivity in an Alaskan fjord. *Sedimentology*, *46*, 1109–26. doi:10.1046/j.1365-3091.1999.00267.x.

Dallmann, W., Ohta, Y., Elvevold, S., & Blomeier, D. (2002). *Bedrock map of Svalbard and Jan Mayen*. Norsk Polarinstitutt, Temakart No. 33.

Dowdeswell, J. A., Elverhøi, A., & Spielhagen, R. (1998). Glacimarine sedimentary processes and facies on the Polar North Atlantic margins. *Quaternary Science Reviews*, *17*, 243–72. doi:10.1016/S0277-3791(97)00071-1.

Dowdeswell, J. A., & Ottesen, D. (2016). Eskers formed at the beds of modern surge-type tidewater glaciers in Spitsbergen. In J. A. Dowdeswell, M. Canals, M. Jakobsson, B. J. Todd, E. K. Dowdeswell, & K. A. Hogan (Eds.), *Atlas of submarine glacial landforms* number 46 in Geological Society Memoir (pp. 83–4). The Geological Society London. doi:10.1144/M46.70.

Dowdeswell, J. A., Whittington, R., Jennings, A., Andrews, J., Mackensen, A., & Marienfeld, P. (2000). An origin for laminated glacimarine sediments through sea-ice build-up and suppressed iceberg rafting. *Sedimentology*, *47*. doi:10.1046/j.1365-3091.2000.00306.x.

Elverhøi, A., Andersen, E., Dokken, T., Hebbeln, D., Spielhagen, R., Svendsen, J., & Forsberg, C. (1995). The growth and decay of the Late Weichselian ice sheet in western Svalbard and adjacent areas based on provenance studies of marine sediments. *Quaternary Research*, *44*, 303–16. doi:10.1006/qres.1995.1076.

Elverhøi, A., Liestøl, O., & Nagy, J. (1980). Glacial erosion, sedimentation and microfauna in the inner part of Kongsfjorden, Spitsbergen. *Norsk Polarinstitutt Skrifter*, *172*, 33–58.

Elverhøi, A., Lønne, Ø., & Seland, R. (1983). Glaciomarine sedimentation in a modern fjord environment, Spitsbergen. *Polar Research*, *1*, 127–50. doi:10.1111/j.1751-8369.1983.tb00697.x.

Evans, D., & Orton, C. (2014). Heinabergsjökull and Skalafellsjökull, Iceland: active temperate piedmont lobe and outwash head glacial landsystem. *Journal of Maps*, *11*, 415–31. doi:10.1080/17445647.2014.919617.

Farnsworth, W. R., Ingólfsson, Ó., Retelle, M., & Schomacker, A. (2016). Over 400 previously undocumented Svalbard surge-type glaciers identified. *Geomorphology*, *264*, 52–60. doi:10.1144/GSL.SP.2002.203.01.09.

Flink, A. E., Noormets, R., Fransner, O., Hogan, K. A., O'Regan, M., & Jakobsson, M. (2017). Past ice flow in Wahlenbergfjorden and its implications for late Quaternary ice sheet dynamics in northeastern Svalbard. *Quaternary Science Reviews*, .

Flink, A. E., Noormets, R., Kirchner, N., Benn, D. I., Luckman, A., & Lovell, H. (2015). The evolution of a submarine landform record following recent and multiple surges of Tunabreen glacier, Svalbard. *Quaternary Science Reviews*, *108*, 37–50. doi:10.1016/j.quascirev.2014.11.006.

Forman, S. (1990). Post-glacial relative sea-level history of northwestern Spitsbergen, Svalbard. *Geological Society of America Bulletin*, *102*, 1580–90. doi:10.1130/0016-7606(1990)102<1580:PGRSLH>2.3.CO;2.

Forwick, M., Baeten, N., & Vorren, T. (2009). Pockmarks in Spitsbergen fjords. *Norwegian Journal of Geology*, *89*, 65–77.

Forwick, M., & Vorren, T. (2007). Holocene mass-transport activity and climate in outer Isfjorden, Spitsbergen: marine and subsurface evidence. *The Holocene*, *17(6)*, 707–16. doi:10.1177/0959683607080510.

Forwick, M., & Vorren, T. (2009). Late Weichselian and Holocene sedimentary environments and ice rafting in Isfjorden, Spitsbergen. *Paleogeography, Paleoclimatology, Paleoecology*, *280(1)*, 258–74. doi:10.1016/j.palaeo.2009.06.026.

Forwick, M., & Vorren, T. (2011). Stratigraphy and deglaciation of the Isfjorden area, Spitsbergen. *Norwegian Journal of Geology*, *90*, 163–79.

Forwick, M., Vorren, T., Hald, M., Korsun, S., Roh, Y., Vogt, C., & Yoo, K. (2010). Spatial and temporal influence of glaciers and rivers on the sedimentary environment in Sassenfjorden and Tempelfjorden, Spitsbergen. *Geological Society, London, Special Publications*, *344(1)*, 163–93. doi:10.1144/SP344.13.

Forwick, M., & Vorren, T. O. (2012). Submarine Mass Wasting in Isfjorden, Spitsbergen. In Y. Yamada, K. Kawamura, K. Ikehara, Y. Ogawa, R. Urgeles, D. Mosher, J. Chaytor, & M. Strasser (Eds.), *Submarine mass movements and their consequences* (pp. 711–22). Springer Springer+ Business Media volume 31. doi:10.1007/978-94-007-2162-3$\textunderscore$63.

Fransner, O., Noormets, R., Flink, A. E., Hogan, K., O'Regan, M., & Jakobsson, M. (2017). Glacial landforms and their implications for glacier dynamics in Rijpfjorden and Duvefjorden, northern Nordaustlandet, Svalbard. *Journal of Quaternary Science*, .

Gilbert, R. (1982). Contemporary sedimentary environments on Baffin Island, NWT, Canada: Glaciomarine processes in fiords of eastern Cumberland Peninsula. *Arctic and Alpine Research*, *14*, 1–12. doi:10.2307/1550809.

Gilbert, R., Aitken, A., & Lemmen, D. (1993). The glacimarine sedimentary environment of Expedition Fiord, Canadian High Arctic. *Marine Geology*, *110*, 257–73. doi:10.1016/0025-3227(93)90088-D.

Gilbert, R., Nielsen, N., Möller, H., Desloges, J., & Rasch, M. (2002). Glacimarine sedimentation in Kangerdluk (Disko Fjord), West Greenland, in response to a surging glacier. *Marine Geology*, *191*, 1–18. doi:10.1016/S0025-3227(02)00543-1.

Hagen, J. (1993). *Glacier atlas of Svalbard and Jan Mayen* volume 129. Norsk Polarinstitutt Middelelser. URL: http://hdl.handle.net/11250/173065.

Hagen, J. O., Kohler, J., Melvold, K., & Winther, J.-G. (2003). Glaciers in Svalbard: mass balance, runoff and freshwater flux. *Polar Research*, *22*, 145–59. doi:10.1111/j.1751-8369.2003.tb00104.x.

Hogan, K. A., Dowdeswell, J. A., Noormets, R., Evans, J., & Ó Cofaigh, C. (2010). Evidence for full-glacial flow and retreat of the Late Weichselian Ice Sheet from the waters around Kong Karls Land, eastern Svalbard. *Quaternary Science Reviews*, *29*, 3563–82. doi:10.1016/j.quascirev.2010.05.026.

Holland, D., Thomas, R., De Young, B., Ribergaard, M., & Lyberth, B. (2008). Acceleration of Jakobshavn Isbræ triggered by warm subsurface ocean waters. *Nature Geoscience*, *1*, 659–64. doi:10.1038/ngeo316.

Hovland, M., & Judd, A. G. (1988). *Seabed pockmarks and seepages: impact on geology, biology and the marine environment*.

Ingólfsson, O., & Landvik, J. (2013). The Svalbard-Barents Sea ice-sheet – historical, current and future perspectives. *Quaternary Science Reviews*, *64*, 33–60. doi:10.1016/j.quascirev.2012.11.034.

Jennings, A. E., & Weiner, N. J. (1996). Environmental change in eastern Greenland during the last 1300 years: evidence from foraminifera and lithofacies in Nansen fjord, 68 °N. *The Holocene*, *6*, 179–91. doi:10.1177/095968369600600205.

Jessen, S., Rasmussen, T., Nielsen, T., & Solheim, A. (2010). A new Late Weichselian and Holocene marine chronology for the western Svalbard slope 30000-0 cal years BP. *Quaternary Science Reviews*, *29(9)*, 1301–12. doi:10.1016/j.quascirev.2010.02.020.

Kehrl, L., Hawley, R., Powell, R., & Brigham-Grette, J. (2011). Glacimarine sedimentation processes at Kronebreen and Kongsvegen, Svalbard. *Journal of Glaciology*, *57(205)*, 841–7. doi:10.3189/002214311798043708.

Kempf, P., Forwick, M., Laberg, J., & Vorren, T. (2013). Late Weichselian – Holocene sedimentary palaeoenvironment and glacial activity in the high-Arctic van Keulenfjorden, Spitsbergen. *The Holocene*, *23(11)*, 1607–18. doi:10.1177/0959683613499055.

King, E., Hindmarsh, R., & Stokes, C. (2009). Formation of mega-scale glacial lineations observed beneath a West Antarctic ice stream. *Nature Geoscience*, *2(8)*, 585–8. doi:10.1038/ngeo581.

Koç, N., Klitgaard-Kristensen, D., Hasle, K., Forsberg, C., & Solheim, A. (2002). Late glacial palaeoceanography of Hinlopen Strait, northern Svalbard. *Polar Research*, *21*, 307–14. doi:10.1111/j.1751-8369.2002.tb00085.x.

Kohler, J., James, T. D., Murray, C. B. O., T.and Nuth, Barrand, N., Aas, H., & Luckman, A. (2007). Acceleration in thinning rate on western Svalbard glaciers. *Geophysical Research Letters*, *34*. doi:10.1029/2007GL030681.

Kristensen, L., Benn, D., Hormes, A., & Ottesen, D. (2009). Mud aprons in front of Svalbard surge moraines: Evidence of subglacial deforming layers or proglacial glaciotectonics? *Geomorphology*, *111(3)*, 206–21. doi:10.1016/j.geomorph.2009.04.022.

Kuenen, P. (1948). Slumping in the Carboniferous rocks of Pembrokeshire. *Quarterly Journal of the Geological Society*, *104*, 365–85. doi:10.1144/GSL.JGS.1948.104.01-04.18.

Landvik, J., Bondevik, S., Elverhøi, A., Fjeldskaar, W., Mangerud, J., Salvigsen, O., Siegert, M. J., Svendsen, J.-I., & O., V. T. (1998). The last glacial maximum of Svalbard and the Barents Sea area: ice sheet extent and configuration.

Quaternary Science Reviews, *17(1-3)*, 43–75. doi:10.1016/S0277-3791(97)00066-8.

Landvik, J., Brook, E., Gualtieri, L., Raisbeck, G., Salvigsen, O., & Yiou, F. (2003). Northwest Svalbard during the last glaciation: Ice-free areas existed. *Geology*, *31*, 905–8. doi:10.1130/G19703.1.

Landvik, J., Ingólfsson, O., Mienert, J., Lehman, S., Solheim, A., Elverhøi, A., & Ottesen, D. (2005). Rethinking Late Weichselian ice-sheet dynamics in coastal NW-Svalbard. *Boreas*, *34(1)*, 7–24. doi:10.1111/j.1502-3885.2005.tb01001.x.

Landvik, J. Y., Hjort, C., Mangerud, J., Moller, P., & Salvigsen, O. (1995). The Quaternary record of eastern Svalbard-an overview. *Polar Research*, *14*, 95–104. doi:10.1111/j.1751-8369.1995.tb00683.x.

Lønne, I., & Mangerud, J. (1991). An Early or Middle Weichselian sequence of proglacial, shallow marine sediments on western Svalbard. *Boreas*, *20*, 85–104. doi:10.1111/j.1502-3885.1991.tb00298.x.

Lovell, T. V. (2000). As climate changes, so do glaciers. *Proceedings of the National Academy of Sciences of the United States of America*, *97*, 1351–4. doi:10.1073/pnas.97.4.1351.

Lundqvist, J. (1981). Moraine morphology. Terminological remarks and regional aspects. *Geografiska Annaler. Series A. Physical Geography*, (pp. 127–38). doi:10.2307/520824.

Mackiewicz, N., Powell, R., Carlson, P., & Molnia, B. (1984). Interlaminated ice-proximal glacimarine sediments in Muir Inlet, Alaska. *Marine Geology*, *57*, 113–47. doi:10.1016/0025-3227(84)90197-X.

Mangerud, J. (1972). Radiocarbon dating of marine shells, including a discussion of apparent age of recent shells from Norway. *Boreas*, *1*, 143–72. doi:10.1111/j.1502-3885.1972.tb00147.x.

Mangerud, J., Bolstad, M., Elgersma, A., Helliksen, D., Landvik, J. Y., Lønne, I., Lycke, A. K., Salvigsen, O., Sandahl, T., & Svendsen, J. I. (1992). The last glacial maximum on Spitsbergen, Svalbard. *Quaternary Research*, *38*, 1–31. doi:10.1016/0033-5894(92)90027-G.

Mangerud, J., & Landvik, J. (2007). Younger Dryas cirque glaciers in western Spitsbergen: smaller than during the Little Ice Age. *Boreas*, *36(3)*, 278–85. doi:10.1111/j.1502-3885.2007.tb01250.x.

Meier, M., & Post, A. (1969). What are glacier surges? *Canadian Journal of Earth Sciences*, *6*, 807–17. doi:10.1139/e69-081.

Ó Cofaigh, C., & Dowdeswell, J. (2001). Laminated sediments in glacimarine environments: diagnostic criteria for their interpretation. *Quaternary Science Reviews*, *20*, 1411–36. doi:10.1016/S0277-3791(00)00177-3.

Ó Cofaigh, C., Dowdeswell, J., Allen, C., Hiemstra, J., Pudsey, C., Evans, J., & Evans, D. (2005). Flow dynamics and till genesis associated with a marine-based Antarctic paleo-ice stream. *Quaternary Science Reviews*, *24*, 709–40. doi:10.1016/j.quascirev.2004.10.006.

Ó Cofaigh, C., Dowdeswell, J., & Grobe, H. (2001). Holocene glacimarine sedimentation, inner Scoresby Sund, East Greenland: the influence of fast-flowing ice-sheet outlet glaciers. *Marine Geology*, *175*, 103–29. doi:10.1016/S0025-3227(01)00117-7.

Oerlemans, J., & Nick, F. (2006). Modelling the advance–retreat cycle of a tidewater glacier with simple sediment dynamics. *Global and Planetary Change*, *50*, 148–60. doi:10.3189/172756407782871440.

Ottesen, D., & Dowdeswell, J. (2006). Assemblages of submarine landforms produced by tidewater glaciers in Svalbard. *Journal of Geophysical Research*, *111*, F01016. doi:10.1029/2005JF000330.

Ottesen, D., & Dowdeswell, J. (2009). An inter-ice stream glaciated margin: submarine landforms and a geomorphic model based on marine-geophysical data from Svalbard. *Geological Society of America Bulletin*, *121(11/12)*, 1647–65. doi:10.1130/B26467.1.

Ottesen, D., Dowdeswell, J., Benn, D., Kristensen, L., Christiansen, H., Christensen, O., & Vorren, T. (2008). Submarine landforms characteristic of glacier surges in two Spitsbergen fjords. *Quaternary Science Reviews*, *27(15)*, 1583–99. doi:10.1016/j.quascirev.2008.05.007.

Ottesen, D., Dowdeswell, J., Landvik, J., & Mienert, J. (2007). Dynamics of the Late-Weichselian ice sheet on Svalbard inferred from high-resolution sea-floor morphology. *Boreas*, *36*, 286–306. doi:10.1111/j.1502-3885.2007.tb01251.x.

Ottesen, D., Dowdeswell, J., & Rise, L. (2005). Submarine landforms and the reconstruction of fast-flowing ice streams within a large Quaternary ice sheet: the 2500-km-long Norwegian-Svalbard margin (57°– 80°N). *Geological Society of America Bulletin*, *117*, 1033–50. doi:10.1130/B25577.1.

Pettersson, R. (2004). *Dynamics of the cold surface layer of polythermal Storglaciären*. Ph.D. thesis Institutionen för naturgeografi och kvartärgeologi.

Plassen, L., Vorren, T., & Forwick, M. (2004). Integrated acoustic and coring investigations of glacigenic deposits in Spitsbergen fjords. *Polar Research*, *23(1)*, 89–110. doi:10.1111/j.1751-8369.2004.tb00132.x.

Powell, R., & Molnia, B. (1989). Glacimarine sedimentary processes, facies and morphology of the south-southeast Alaska shelf and fjords. *Marine Geology*, *85*, 359–90. doi:10.1016/0025-3227(89)90160-6.

Raymond, C. (1987). How do glaciers surge? A review. *Journal of Geophysical Research: Solid Earth (1978-2012)*, *92(B9)*, 9121–34. doi:10.1029/JB092iB09p09121.

Reimer, P., Bard, E., Bayliss, A., Beck, J., Blackwell, P., Ramsey, C., Buck, C., Cheng, H., Edwards, R., Friedrich, M., Grootes, P., Guilderson, T., Haflidason, H., Hajdas, I., Hatté, C., Heaton, T., Hoffmann, D., Hogg, A., Hughen, K., Kaiser, F., Kromer, B., Manning, S., Niu, M., Reimer, R., Richards, D., Scott, E., Southon, J., Staff, R., Turney, C., & van der Plicht, J. (2013). IntCal13 and Marine13 Radiocarbon Age Calibration Curves 0–50,000 Years cal BP. *Radiocarbon*, *55*, 1869–87. doi:10.2458/azu$\textunderscore$js$\textunderscore$rc.55.16947.

Roy, S., Hovland, M., Noormets, R., & Olaussen, S. (2015). Seepage in Isfjorden and its tributary fjords, West Spitsbergen. *Marine Geology*, *363*, 146–59. doi:10.1144/GSL.SP.1993.070.01.06.

Roy, S., Senger, K., Braathen, A., Noormets, R., Hovland, M., & Olaussen, S. (2014). Fluid migration pathways to seafloor seepage in inner Isfjorden and Adventfjorden, Svalbard. *Norwegian Journal of Geology*, *94*, 99–119. URL: http://hdl.handle.net/1956/10661.

Senger, K., Roy, S., Braathen, A., Buckley, S. J., Bælum, K., Gernigon, L., Mjelde, R., Noormets, R., Ogata, K., Olaussen, S., Planke, S., Ruud, B., &

Tveranger, J. (2013). Geometries of doleritic intrusions in central Spitsbergen, Svalbard: an integrated study of an onshore-offshore magmatic province with implications for CO2 sequestration, . *93*, 143–6.

Sexton, D. J., Dowdeswell, J. A., Solheim, A., & Elverhøi, A. (1992). Seismic architecture and sedimentation in northwest Spitsbergen fjords. *Marine Geology*, *103*, 53–68. doi:10.1016/0025-3227(92)90008-6.

Sharp, M. (1985). Crevasse-fill-ridges - a landform type characteristic of surging glaciers? *Geografiska Annaler. Series A. Physical Geography*, *67(3/4)*, 213–20. doi:10.2307/521099.

Sharp, M. (1988). Surging glaciers: behaviour and mechanisms. *Progress in Physical Geography*, *12(3)*, 349–70. doi:10.1177/030913338801200302.

Solheim, A. (1991). The depositional environment of surging sub-polar tidewater glaciers. *Norsk Polarinstitutt Skrifter*, *194*, 1–97.

Solheim, A., & Pfirman, S. (1985). Sea-floor morphology outside a grounded, surging glacier; Bråsvellbreen, Svalbard. *Marine Geology*, *65*, 127–43. doi:10.1016/0025-3227(85)90050-7.

Stewart, F. S., & Stoker, M. S. (1990). Problems Associated with Seismic Facies Analysis of Diamicton-Dominated, Shelf Glacigenic Sequences. *Geo-Marine Letters*, *10*, 151–6. doi:10.1007/BF02085930.

Streuff, K. (2013). *Landform assemblages in inner Kongsfjorden, Svalbard: Evidence of recent glacial (surge) activity*. Master's thesis University of Tromsø.

Streuff, K., Forwick, M., Szczuciński, W., Andreassen, K., & Ó Cofaigh, C. (2015). Landform assemblages in inner Kongsfjorden, Svalbard: evidence of recent glacial (surge) activity. *Arktos*, *1*. doi:10.1007/s41063-015-0003-y.

Streuff, K., Ó Cofaigh, C., Noormets, R., & Lloyd, J. (2017). Submarine landforms and glacimarine sedimentary processes in Lomfjorden, east Spitsbergen. *Marine Geology*, . doi:10.1016/j.margeo.2017.04.014.

Svendsen, J., Elverhøi, A., & Mangerud, J. (1996). The retreat of the Barents Sea Ice Sheet on the western Svalbard margin. *Boreas*, *25*, 244–56. doi:10.1111/j.1502-3885.1996.tb00640.x.

Svendsen, J., Mangerud, J., Elverhøi, A., Solheim, A., & Schüttenhelm, R. (1992). The Late Weichselian glacial maximum on western Spitsbergen inferred from offshore sediment cores. *Marine Geology*, *104*, 1–17. doi:10.1016/0025-3227(92)90081-R.

Syvitski, J., Andrews, J., & Dowdeswell, J. (1996). Sediment deposition in an iceberg-dominated glacimarine environment, East Greenland: basin fill implications. *Global and Planetary Change*, *12*, 251–70. doi:10.1016/0921-8181(95)00023-2.

Syvitski, J. P. M. (1989). On the deposition of sediment within glacier-influenced fjords: oceanographic controls. *Marine Geology*, *85*, 301–29. doi:10.1016/0025-3227(89)90158-8.

Tulaczyk, S., Scherer, R., & Clark, C. (2001). A ploughing model for the origin of weak tills beneath ice streams: a qualitative treatment. *Quaternary Internationals*, *86*, 59–70. doi:10.1016/S1040-6182(01)00050-7.

Velle, J. (2012). *Holocene sedimentary environments in Smeerenburgfjorden, Spitsbergen*. Master's thesis University of Tromsø.

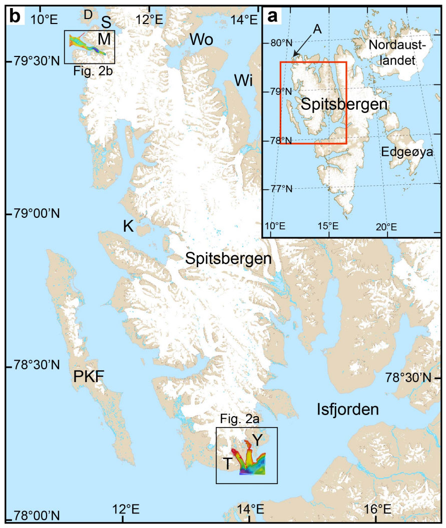

Figure 1: a) Overview of the Svalbard archipelago and its main islands. A = Amsterdamøya. The red rectangle shows the extent of b) map of the central and northwestern coast of Spitsbergen, with bathymetry coverage available for this study. Y = Ymerbukta, T = Trygghamna, PKF = Prins Karls Forland, K = Kongsfjorden, M = Magdalenefjorden, D = Danskøya, Wo = Woodfjorden, Wi = Wijdefjorden. Map data courtesy of the Norwegian Polar Institute.

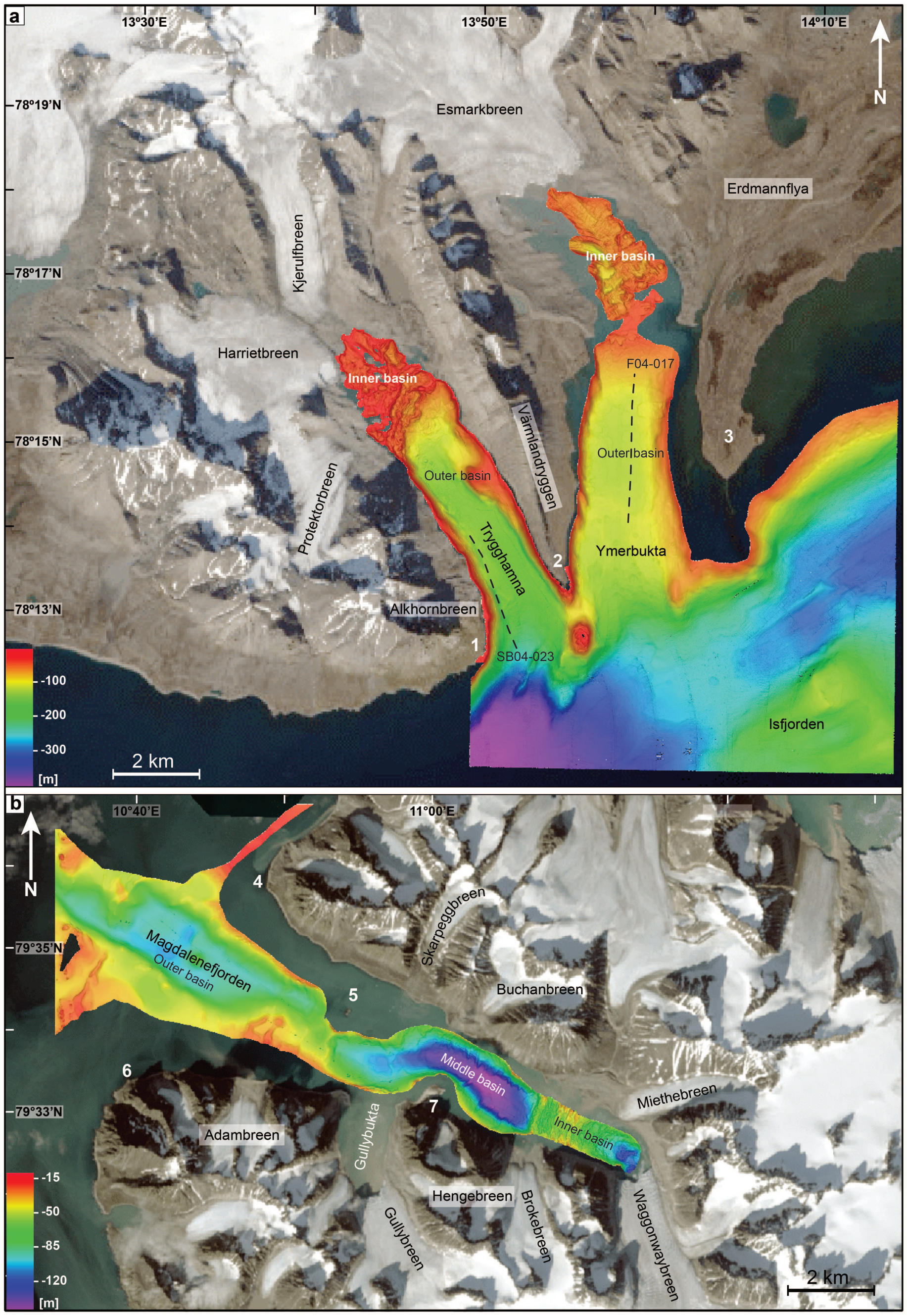

Figure 2: a) Ymerbukta and Trygghamna with their surroundings and the bathymetric data available from the two fjords. 1 = Alkepynten, 2 = Selmaneset, 3 = Erdmannodden. Dashed lines indicate the location of sparker and boomer profiles F04-163 and SB04-023, which were visualised and interpreted in Forwick & Vorren (2011, 2012) and provide the basis for the seismostratigraphy in Ymerbukta and Trygghamna. b) Magdalenefjorden, its surroundings, and the bathymetric data available for this study. 4 = Knattodden, 5 = Fugleholmen, 6 = Magdalenehuken, 7 = Gravneset. For an overview of the study areas' location see also Figure 1. The water depth scale is the same for all subsequent figures.

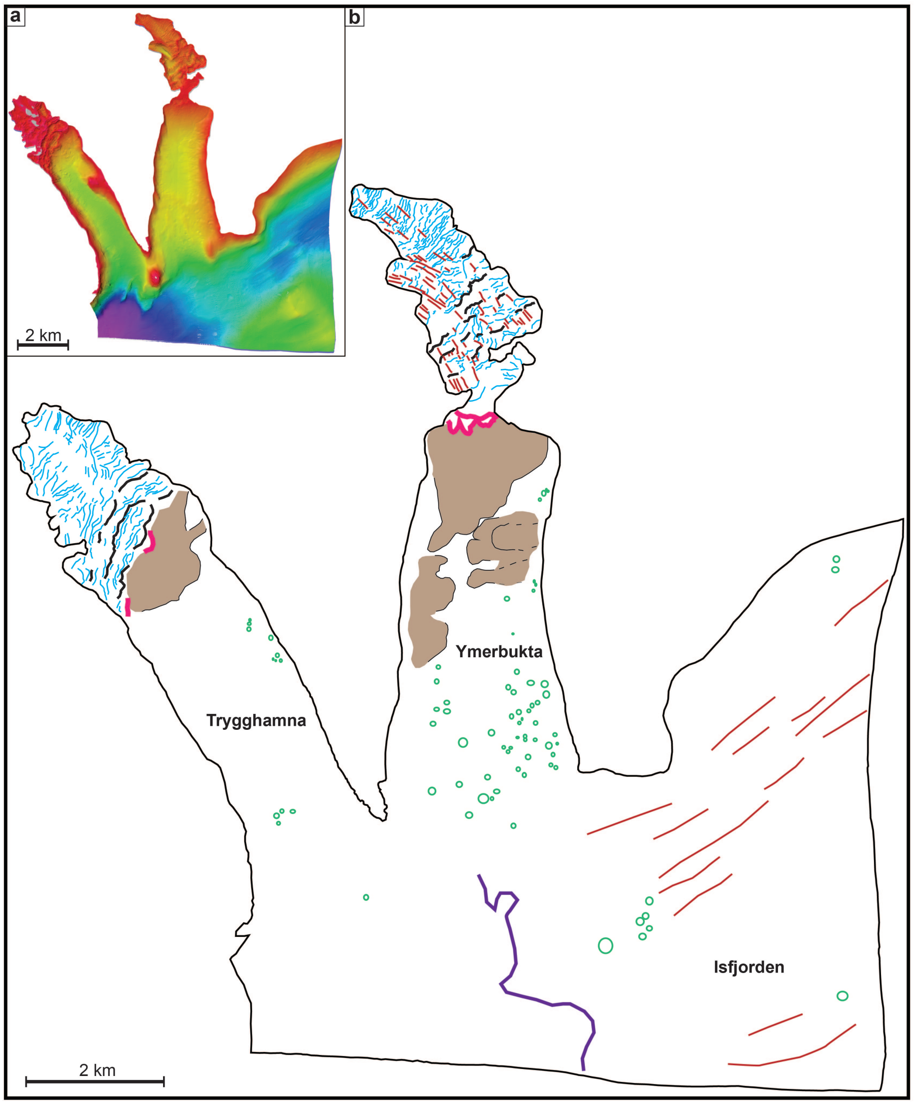

Figure 3: a) Swath-bathymetric data from Ymerbukta and Trygghamna. For the depth scale refer to Figure 2. b) Geomorphological map of the landforms in Ymerbukta, Trygghamna and parts of Isfjorden. Pockmarks and debris lobes were previously described and interpreted by Forwick et al. (2009); Forwick & Vorren (2012).

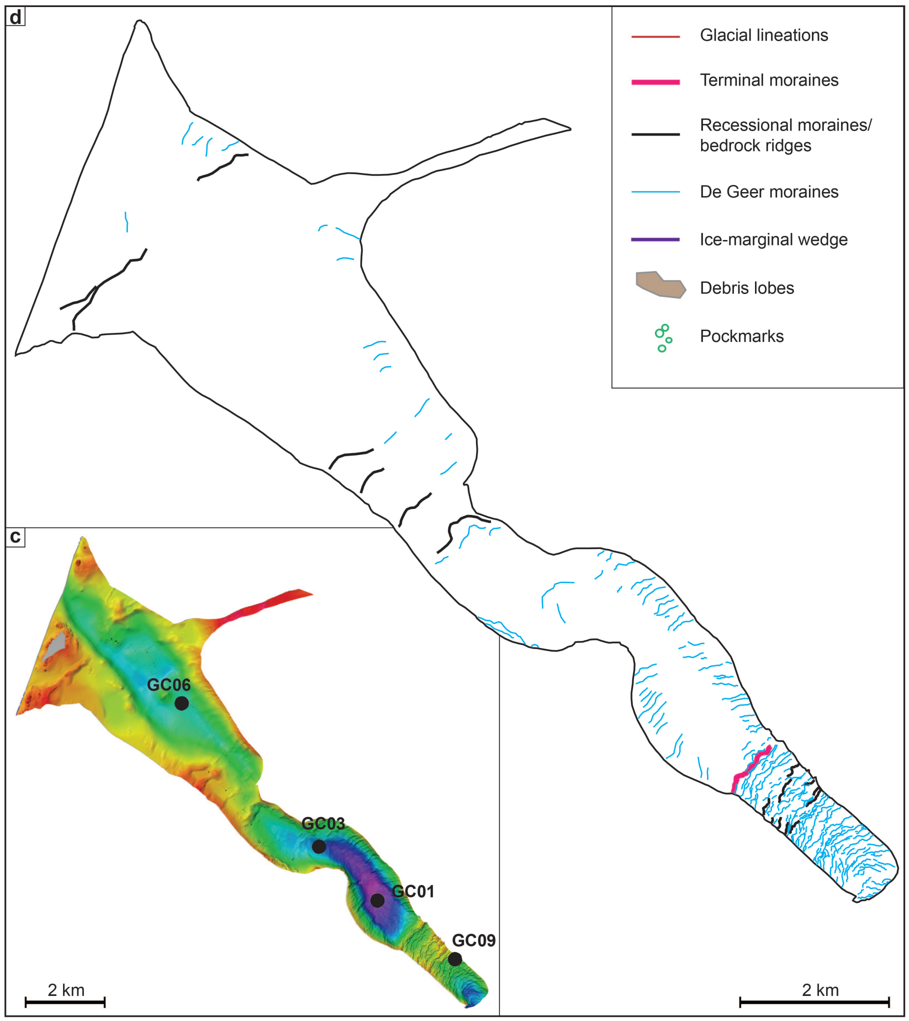

Figure 3 (cont.): c) Swath-bathymetric data with indicated core locations from Magdalenefjorden. For the water depth scale refer to Figure 2. d) Geomorphological map of the landforms in Magdalenefjorden. Part of the moraines/bedrock ridges in the outer and central fjord have been previously documented and interpreted by Ottesen & Dowdeswell (2009).

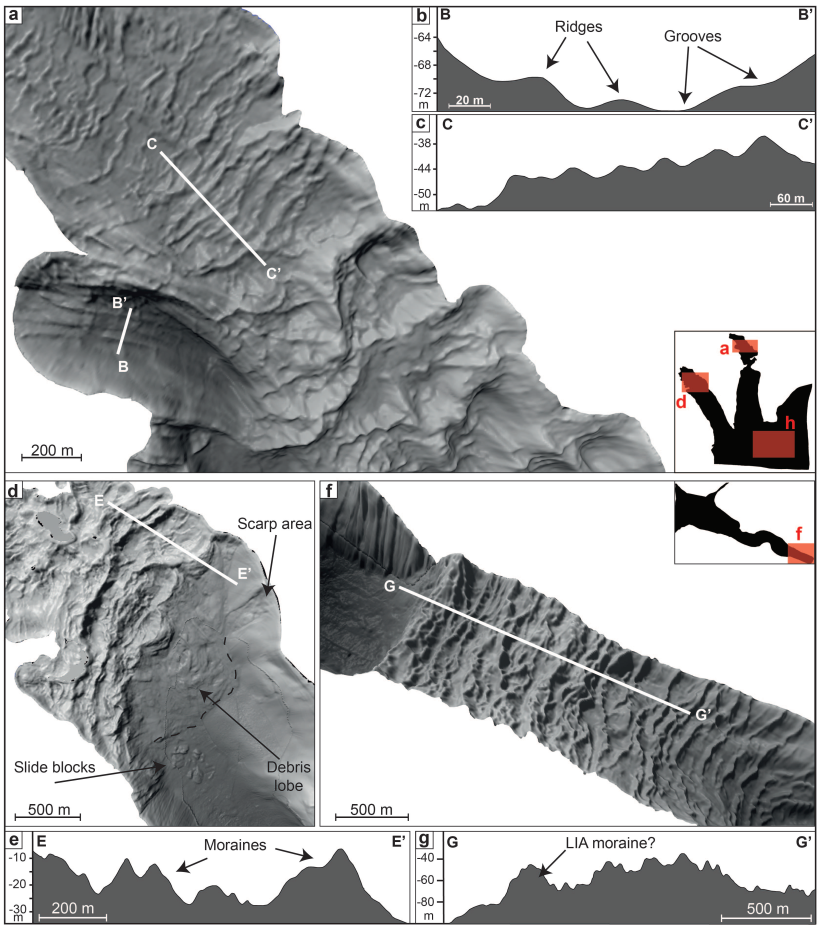

Figure 4: a) Seafloor of the inner fjord basin of Ymerbukta, showing examples of glacial lineations and De Geer moraines. Small red rectangles on the black polygon indicate the location of the subfigures a), d), and h). b) and c) show the cross-sectional profiles B–B' and C–C' across the landforms, respectively. d) Large transverse moraines and an associated debris lobe in Trygghamna. e) Cross-sectional profiles E–E' across Trygghamna moraines. f) De Geer moraines in Magdalenefjorden with g) cross-sectional profile G–G' across them.

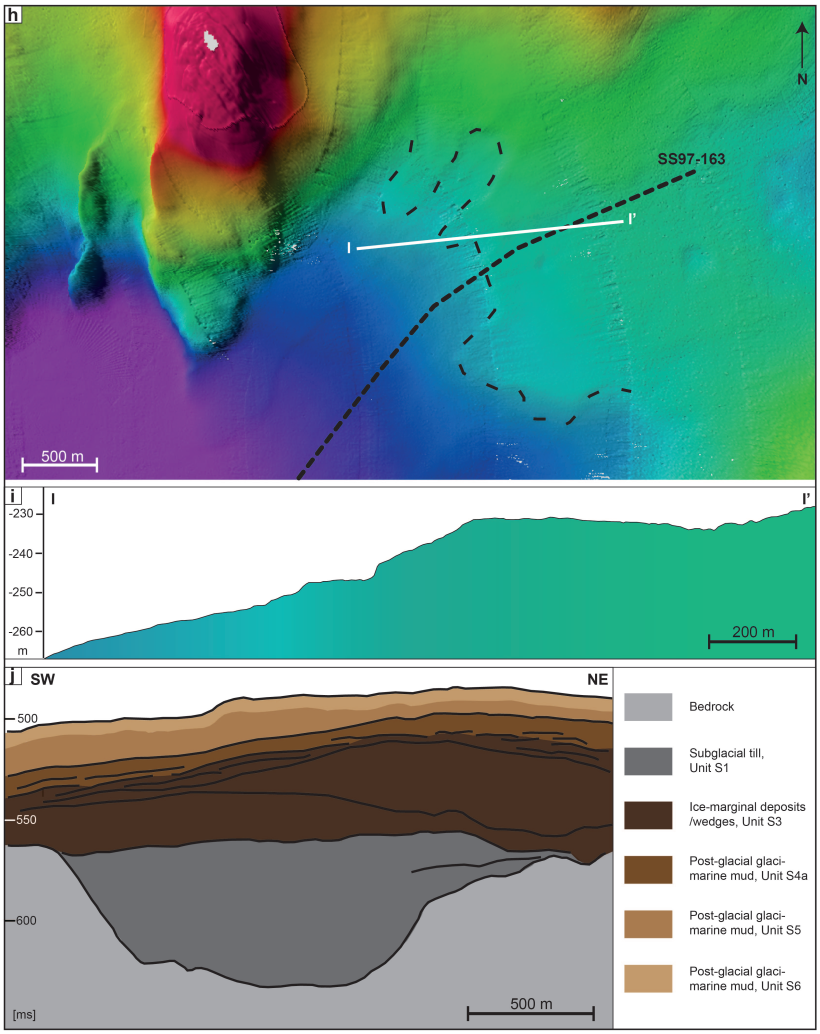

Figure 4 (cont.): h) Ice-marginal deposit in Isfjorden, with i) showing the cross-sectional profile I–I'. For water depth scale please refer to Figure 2. j) Acoustic facies interpretation of seismic line SS97-163 (based on, and modified after Forwick & Vorren, 2011). Y-axis shows two-way travel time in ms.

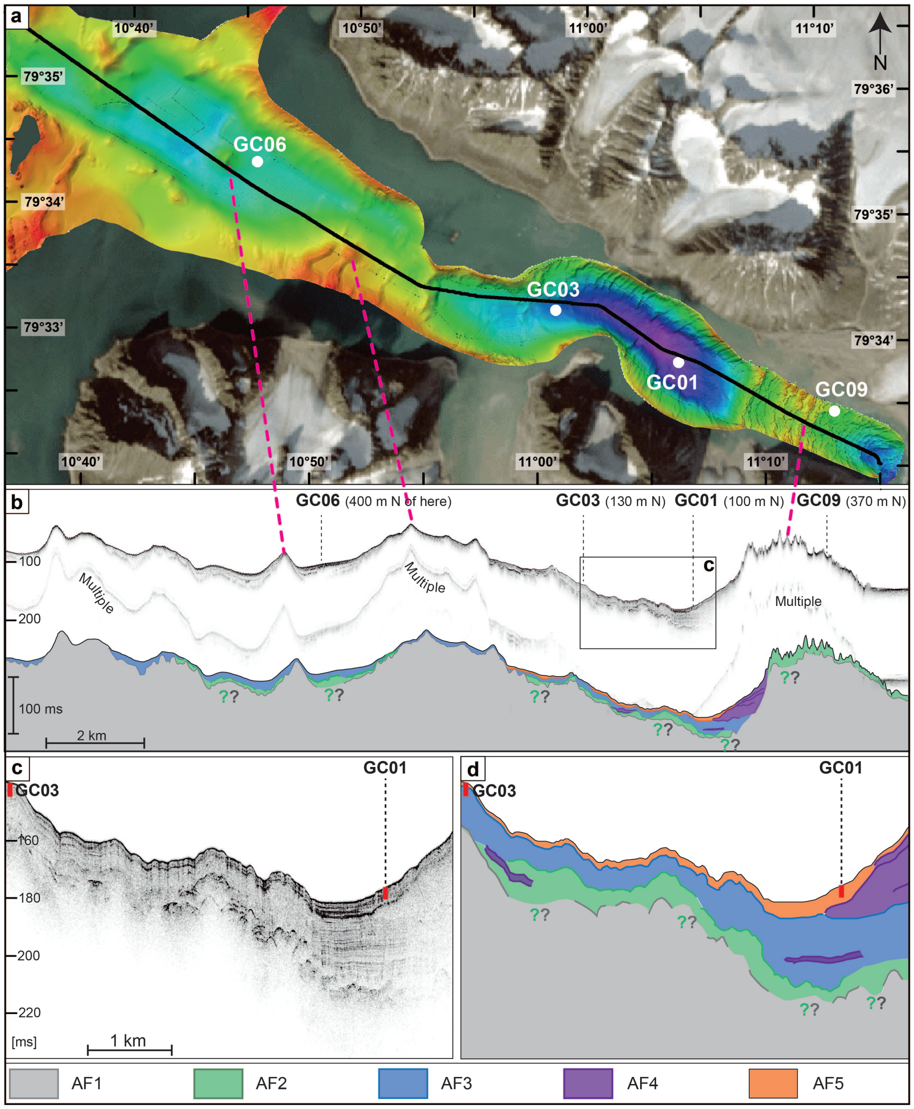

Figure 5: a) Bathymetry in Magdalenefjorden with the location of all cores (white dots) and chirp line 09JM-AG211-006 (black line) indicated. b) Seismic profile of chirp line 006, with approximate locations of the gravity cores. Pink stippled lines correlate bathymetric ridges with the according highs on the seismic profile. The interpretation of the acoustic facies in Magdalenefjorden is shown underneath the seismic profile. The black rectangle marks the extent of c). c) Detailed excerpt from chirp line 006 (black rectangle in b) showing examples of the acoustic facies in Magdalenefjorden. d) Acoustic facies interpretation of c). Red lines in c) and d) illustrate how far GC01 and GC03 penetrate into the seafloor sediments and how they correlate with the acoustic facies in the fjord. Y-axes show two-way travel time in ms.

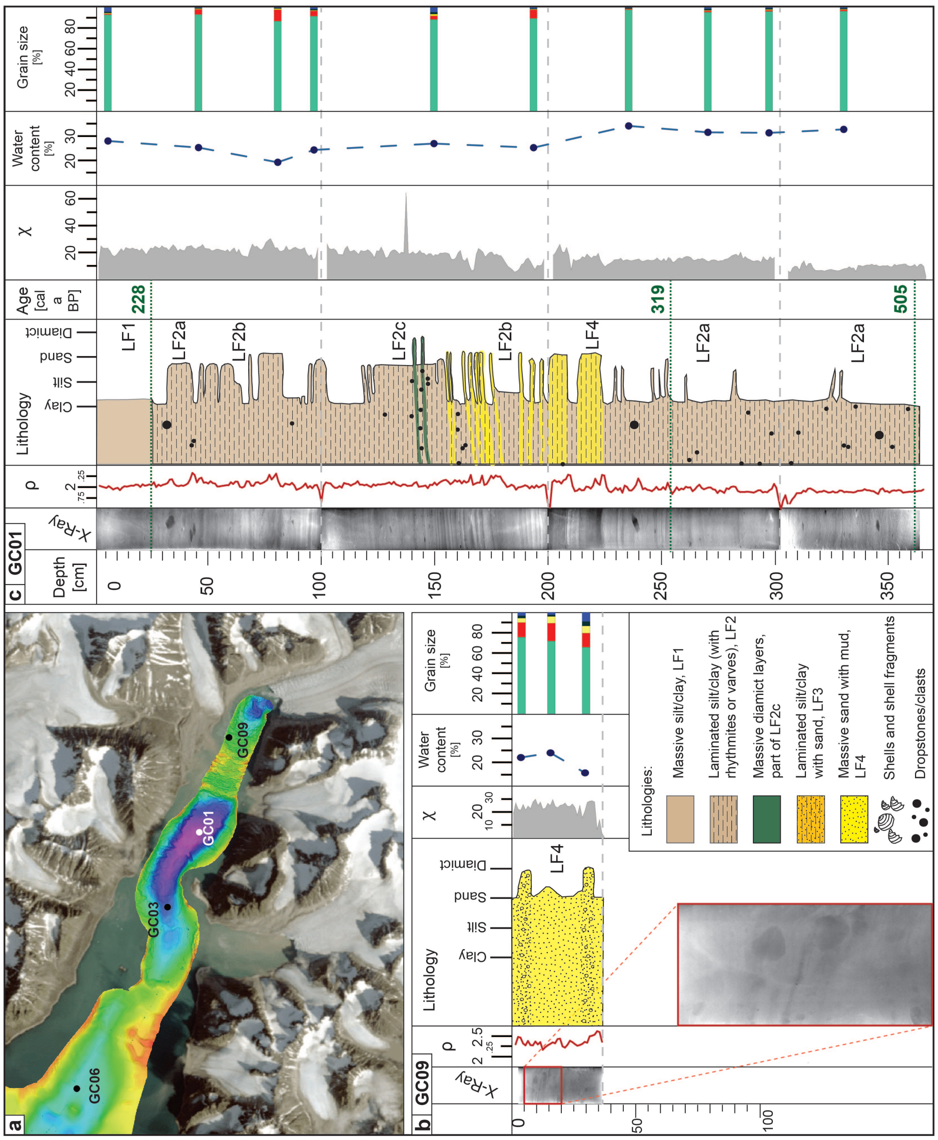

Figure 6: a) Overview of the four core locations in Magdalenfjorden with respect to the bathymetry. b) X-radiographs, lithofacies log and physical properties of core GC09 in the inner fjord. ρ = wet bulk density, χ = magnetic susceptibility in SI x 10^{-5}. c) X-radiographs, lithofacies log and physical properties of core GC01 in the central fjord.

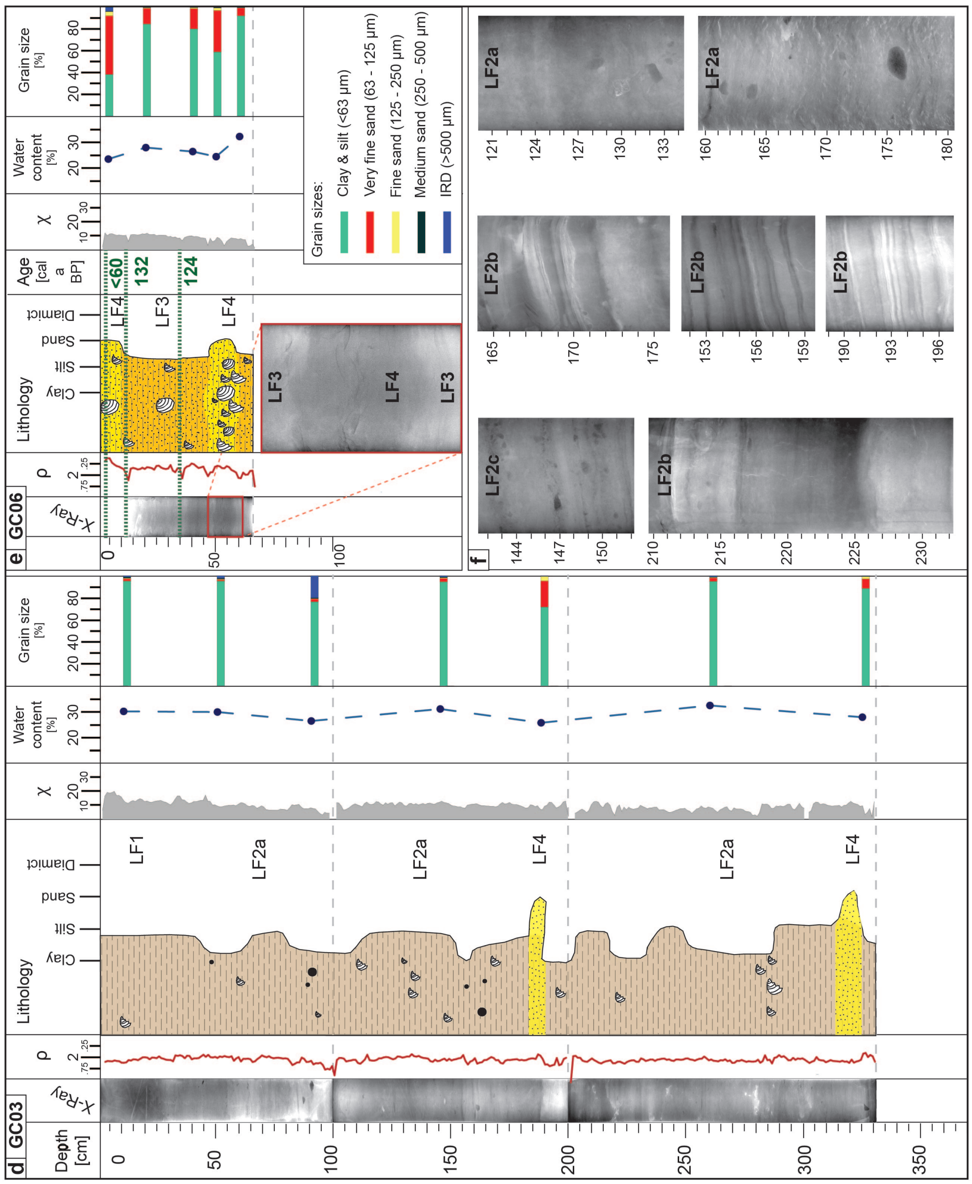

Figure 6 (cont.): d) X-radiographs, lithofacies log and physical properties of core GC03 in the central fjord. e) X-radiographs, lithofacies log and physical properties of core GC06 in the outer fjord. f) Examples of the x-radiographs showing the different types of laminated/stratified sediment in Magdalenefjorden.

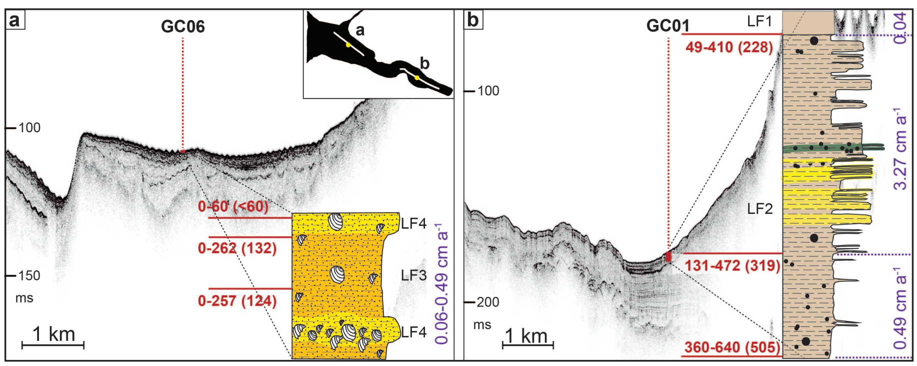

Figure 7: a) Detail of chirp line 09JM-AG211-003 with core location and log of GC06. White lines and dots on the black polygon in the top-right hand corner show the locations of a and b with respect to the bathymetric outline. b) Detail of chirp line 09JM-AG211-006 with the core location and log of GC01. Red lines and numbers show the 2-σ range and the median radiocarbon age in brackets at respective sediment depths, while purple labels refer to sediment accumulation rates. Y-axes show two-way travel time in ms.